Dissertation
submitted to the
Combined Faculties for the Natural Sciences and for Mathematics
of the Ruperto–Carola University of Heidelberg, Germany
for the degree of
Doctor of Natural Sciences

Put forward by
Dipl. Engineer: Gonzalo A. Cabal A.
Born in: Pereira, Colombia
Oral examination: July 11, 2012

Novel methods for treatment planning in Ion Beam Therapy

Referees: **Prof. Dr. Uwe Oelfke**

Prof. Dr. Oliver Jäkel

Abstract

One of the biggest challenges in ion beam therapy is the mitigation of the impact of uncertainties in the quality of treatment plans. Some of the strategies used to reduce this impact are based on concepts developed decades ago for photon therapy. In this thesis novel methods and concepts, tailored to the specific needs of ion beam therapy, are proposed which reduce the effect of uncertainties on treatment plans. This is done in two steps: First, we revisit the concept of the Planning Target Volume and propose a novel method for its definition. This method enhances robustness of treatment plans and reduces the amount of healthy tissue irradiated. In a clinical situation this could translate into an enhancement of the tumor control probability while reducing side effects. The concept of robust conformity (conformity in the presence of uncertainties) is proposed along with a way to quantify it. Secondly,a method to select robust beam angle configurations that also spare organs at risks is proposed. This combination is a new conceptual layout to tackle the challenges of ion beam therapy and enhances its potential.

Zusammenfassung

Eine der größten Herausforderungen in der Ionenstrahltherapie ist die Beschränkung der Einflüsse von Ungenauigkeiten in der Therapieplanung. Einige Strategien, die verwendet werden, um diese Effekte zu verringern, basieren auf Konzepten die vor Jahrzehnten für die Photonentherapie entwickelt wurden. In der vorliegenden Arbeit werden neue Methoden und Konzepte vorgestellt, die speziell auf die Anforderungen der Ionenstrahltherapie zugeschnitten sind und die Auswirkungen von Ungenauigkeiten auf die Therapieplanung verringern. Dies erfolgt in zwei Schritten: Zuerst untersuchen wir das Konzept des geplanten Targetvolumens und schlagen eine neue Definition hierfür vor. Diese erhöht die Robustheit der Therapieplanung und reduziert die Menge von gesundem Gewebe, das bestrahlt wird. In klinischen Anwendungen kann dies die Tumorkontrollrate erhöhen, während gleichzeitig Nebenwirkungen verringert werden. Das Konzept der robusten Konformität (Konformität bei vorliegenden Ungenauigkeiten) wird zur Quantifizierung dieser Verbesserungen vorgeschlagen.

Im zweiten Schritt schlagen wir, aufbauend auf die Konzepte, die im ersten Teil eingeführt wurden, eine Methode vor, mit der robuste Kombinationen von Strahlrichtungen ausgewählt werden knnen, die auerdem Risikoorgane vermeiden. Die Verknüpfung dieser beiden Schritte stellt ein neues Konzept dar, das die Herausforderungen der Ionenstrahltherapie überwinden kann und damit das Potential dieser Therapie erhöht.

A mi padre,
por su admirable ejemplo de responsabilidad y entrega,
en su cumpleaños.

Acknowledgements

"One can never pay in gratitude; one can only pay "in kind" somewhere else in life..."

Anne Morrow Lindbergh

First I would like to thank Prof. Dr. Oliver Jäkel for allowing me to be part of his research group at the German Cancer Research Center for the last three years.

I would also like to thank Prof. Dr. Shuang Luan from the University of New Mexico, not only for hosting me in his institution for a period of five weeks, but also and most important for his kindness, his support and his valuable discussions and advises.

To Dr. David Arboleda from Universidad de Antioquia and Dr. Ilaria Rinaldi, Dr. Andrea Mairani and Prof. Dr. Katia Parodi from the Heidelberg Ion Beam Therapy Center I thank for their support, their friendship and their encouragement over the last years.

To my colleages at the E0409 group of DKFZ and specially to Dr. Harald Latzel, Dr. Franz Joachim Kaiser, Dr. Steffen Greilich, Dipl. Phys. Nora Hünemohr and Dr. Michael Holzscheiter, I am grateful for their help on daily issues. They were not few the times in which their assistance allowed me to get through the day.

To Prof. Dr. Hartmut Dickhaus and Dr. Roland Metzner I am grateful for giving me the chance to spend several months in Chile. During this time I had the pleasure of working with Prof. Beatriz Sanchez and her group at the Pontificia Universidad Catolica de Chile. Her kindness and disposition were verz helpful during the time that this manuscript was being written. I also want to thank Dr. Walter Eckel, Isabel Aliaga Rosson and Johanna Köhl from the Heidelberg Center for Latin America for their help and assistance during my time in Chile.

Finally, I want to thank my mother Norma, my father Alfonso and my brother Nicolas. They have been the moral support in times of sun and rain. I am looking forward to having them close, again.

Contents

List of Figures

List of Tables

Preface

The work presented in this thesis deals with the problem of robustness in ion beam treatment plans. There are many directions from which this problem can be tackled or at least, studied. This work focuses on two of them: First is the concept of planning target volume as a way to assure robust dose coverage in the target. The second is the selection of beam angles as a way to provide robust plans while taking into account sensitive structures.

Both works are built over the concept of *Dynamic Target Definition* which is presented and developed in Chapter 2. Chapter 3 uses some of these concepts to propose a way to develop criteria for robust beam angle selections. More than just offering algorithms to achieve a certain goal, the work presented in Chapters 2 and 3 introduces a new conceptual layout for robust treatment planning. Chapter 4 rounds up this work with a discussion and a summary of the conclusions as well as giving an outlook on the topics that are left for further investigation.

In order to work and develop a study on concepts and algorithms for treatment planning is mandatory to have a Treatment Planning System (TPS). Very few groups nowadays have access to well documented, open sourced TPS to investigate and develop new methods. A significant amount of time was spent by the author of this work to develop a software that could be used as a platform for his treatment planning studies. The result of such effort is *PartPlan*, a set of scripts developed for the Maltab computational environment((MATLAB 7.7, The MathWorks Inc., Natick, MA, 2010)) having functionalities similar to what is found in a TPS.

PartPlan reads in CT data in the format used in Virtous software (1). It performs dose calculations for proton and ion beams based on a Ray-Tracing-WEPL algorithm, it does treatment plan optimization and RBE-weighted optimization as presented in this chapter. In addition it calculates the biological effect using precalculated α and β of the LQ model for a set of pristine Bragg peaks and uses them to get an estimate of the effect using equations 1.17 and 1.18 [1].

[1] At the moment only data for Human Salivary Gland (HSG) cells is available in the system.

To finalize, it is stated that the material presented in Chapter 2 was presented in oral contributions in three international conferences:

- XVIth International Conference of the Use of Computers in Radiation Therapy, May 2010,Amsterdam, Holland.(2)
- 50^{th} Annual Particle Therapy Cooperative Group Meeting, May 2010, Chiba, Japan.(3)
- 51^{th} Annual Particle Therapy Cooperative Group Meeting, May 2011, Philadelphia, PE, USA.(4)

It was partly published on the *Proceedings of the XVI^{th} International Conference of the Use of Computers in Radiation Therapy, Amsterdam, Holland*(2). It was submitted for publication and conditionally accepted under the tittle: *Dynamic Target Definition: A novel approach for ion beam therapy*(5) in *Radiotherapy and Oncology.*

Part of the material presented in Chapter 3 was presented in one international conference:

- 49^{th} Annual Particle Therapy Cooperative Group Meeting, September 2009, Heidelberg, Germany. (6, 7)

A manuscript with the methods and results presented in Chapter 3 is ready and it will be submitted as soon as the first manuscript is available on line, as it is strongly based on the concepts developed in it.

This project was funded by the Helmholtz Association under the contract number VH-VI-303.

Gonzalo A. Cabal A.

1

Introduction

"It must have occurred to many people that the particles themselves now become of considerable therapeutic interest."(8)

The scenario is the post-war America, the year is 1946. Like others brilliant scientist of his time, Robert Rathbun Wilson belonged to a group of physicist that shared three things. First, they were part of the generation that followed the golden years of modern physics. It was a generation that had the enormous task of realizing important technical and experimental developments after major shifts in paradigms in physics had taken place just few years ago. Second, he belonged to a selected group of talented young people who took part in the Manhattan Project. And finally, he was also among those who, after the war, were very concerned about the military applications of nuclear power. In the America of 1946, there were voices already claiming for peaceful applications of nuclear research.

After the war was over, Wilson accepted a short appointment at the Harvard Cyclotron Laboratory. While taking part in the design of the shielding for the cyclotron he realized that protons could potentially be used as a radiotherapeutic modality and this idea was published in 1946 under the title "Radiological use of fast protons"(8). The idea was so simple and elegant, that in an act of humbleness and modesty, his did not even attempt to present it as his own:

> "It must have occurred to many people that the particles themselves now become of considerable therapeutic interest. The object of this paper is to

acquaint medical and biological workers with some of the physical properties and possibilities of such rays." (8)

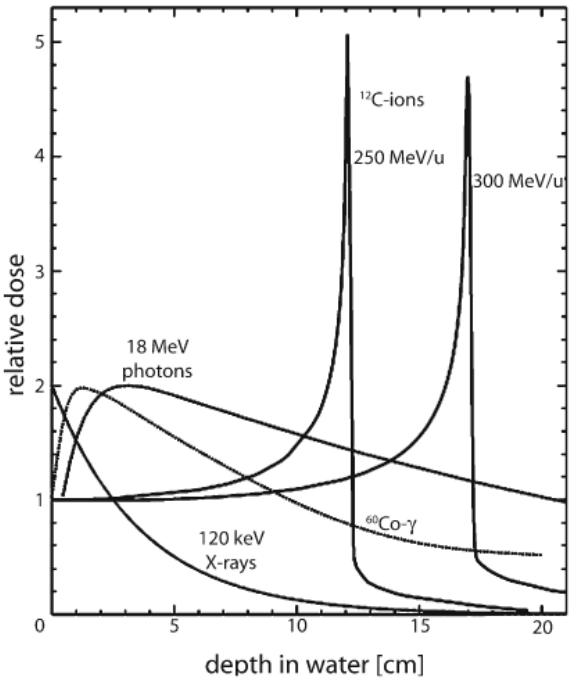

Figure 1.1: Depth dose curves for different radiation modalities - Bragg peaks for carbon ion beams and depth dose curve for x-ray fields is shown. Taken from (9)

This is considered to be the seminal paper for proton therapy and in the America of the post-war these ideas resonated, they bloomed.

The first patients were treated in physics laboratories. In 1954 the first ion beam treatments were delivered with protons in Berkeley (10). Three years later proton treatments began in Uppsala, Sweden (11). During the 60's and 70's several research facilities in Russia and Japan started treatments with protons. In 1961 treatments began at the Harvard Cyclotron Laboratory in collaboration with the Massachusetts General Hospital. In 1990 the first hospital based proton therapy facility was built in Loma Linda University Medical Center (LLUMC) in Loma Linda, California and some years later the Massachusetts General Hospital opened its fully hospital based proton program. Nowadays more than a dozen of ion beam facilities for proton and heavy ion therapy have been built and a good number are either under planning or under

construction. In Germany, the experience from the Pilot Project carried out at the Gesellschaft für Schwerionenforschung (GSI) in collaboration with the German Cancer Research Center (DKFZ) and the University Hospital of Heidelberg led to the creation of the Heidelberg Ion Beam Therapy Center (HIT) and its currently treating patients with protons and carbon ion beams. Other facilities in Munich and Berlin offer proton therapy.

1.1 Dose delivery in ion beam therapy: Active and passive systems

Generally speaking the machine for ion beam therapy is composed of three main parts. One part locates the ion sources, the hardware required to inject the particles into the accelerator and the accelerator itself. This accelerator is either a cyclotron or a synchrotron. The second part of the system transports the accelerated ions into the treatment rooms. The last part of the system is is what is used to deliver the beam. The most important elements for dose delivery are located in this third part. There are two ways in which the dose can be delivered to the patient, we will refer to them as *active and passive systems.*

The passive system is right now the most common modality of dose delivery. Some of its design was already suggested by Wilson in his seminal paper. He wrote:

> "In treating large tumors, for example, one will want to cover the whole volume with the very high ionization density which obtains over the last few millimeters. This can easily be accomplished by interposing a rotating wheel of variable thickness, corresponding to the tumor thickness, between the source and the patient."(8)

It is remarkable that in this early paper the use of a modulating wheel is already proposed. However in order to make a passive system more elements are needed. Very briefly, the main components of a passive delivery system are:

Scattering device(s) : In order to use ion beams therapeutically they must be broaden to cover field sizes up to 20-25 cm. For small field sizes such as the ones used for uveal melanoma irradiations, a single scattering foil is sufficient.

A high density material, like lead, is usually used. For bigger field sizes a double scattering system is used. It consist of a set of foils usually referred to as first scatterer (placed near the nozzle entrance) and a second scatterer usually gaussian shaped (placed further downstream). A very complete discussion on the scattering physics and the design of the scattering devices can be found in (12).

Modulator wheel : As suggested by Wilson (8), it is made of set of absorbers of different thickness placed on a wheel. By rotating the wheel each of the absorbers will meet the beam reducing the range of the monoenergetic particles. By combining the different pristine Bragg peaks obtained with each of the absorbers of the wheel the Spread Out Bragg Peak (SOBP) is generated. Very often the wheel is made of a combination of low-Z materials and high-Z materials. The low-Z materials slow down the particles with minimal scattering while the high-Z materials spread out the beam at each depth.

Collimators and apertures : They shape the field to the adequate profile. The material often used is brass.

Compensator : It adjusts the distal part of the dose distribution to conform the shape of the target. Compensators and apertures are patient and field specific hardware.

In the passive delivery system the dose is delivered simultaneously to the plane perpendicular to the direction of the beam at a given depth (thanks to the scatterers) and within fractions of seconds to the whole volume (by using the modulator wheel).

The active delivery system carefully locates the beam spots one at the time over the whole target. In order to control the depth (or range) of the particle, the energy of the beam is adjusted either by the accelerator itself (in the case of the synchrotron) or by placing a slab of material to slow down the beam (as it is done for cyclotrons). In order to move the beam spot off the central axis two approaches have been implemented clinically. At GSI a set of magnets,usually called scanning magnets, allows to locate the particle at any position in the transversal plane (14). A representation of this design is show in Figure 1.3. At the Paul Scherrer Institute (PSI) in Switzerland, a wobbler magnet laterally deflects the particles in directions parallel to the x-z plane (13). The

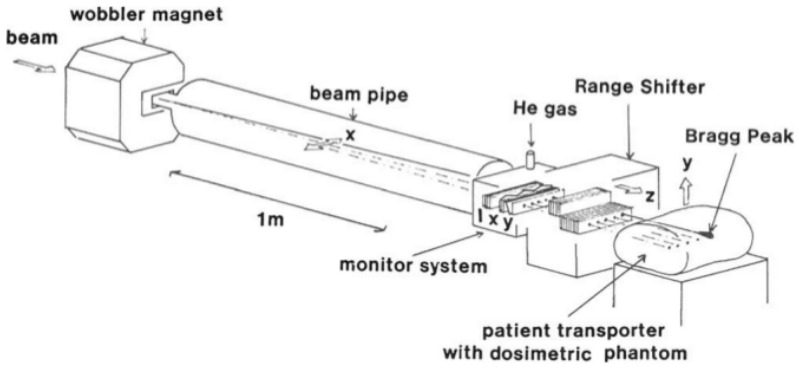

Figure 1.2: Active delivery system at PSI - Schematic representation of the active delivery system used at the Paul Scherrer Institute (PSI) in Switzerland. Taken from (13)

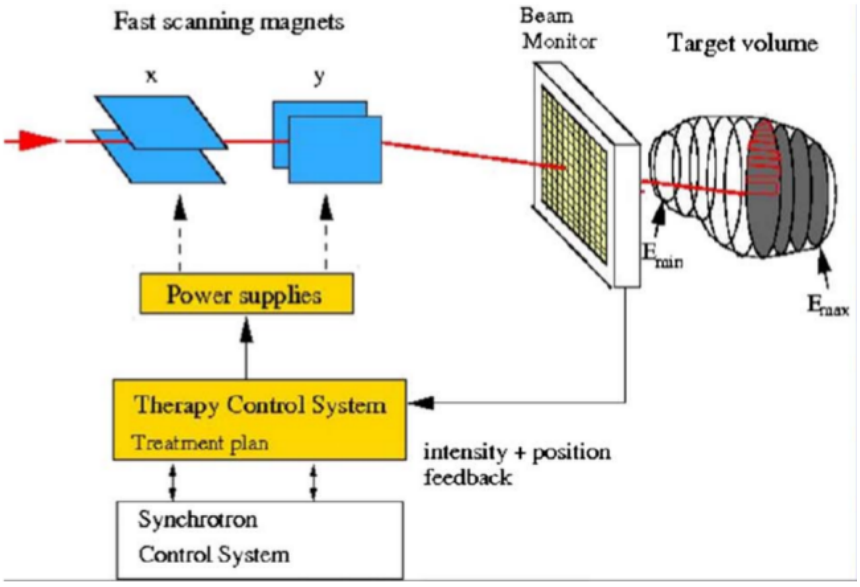

Figure 1.3: Active delivery system at HIT/GSI - Schematic representation of the active delivery system used at Heidelberg Ion Beam Therapy Center in Germany. Taken from (14)

location of the spot in the y-component is achieved by moving the treatment table. Figure 1.2 shows the schematics of the design.

The two systems have different advantages and disadvantages. In the case of passive systems, these are remarkable robust and stable; commissioning and quality assurance are much simpler than for active systems and are generally well understood thanks to more than half of century of use and experience. On the negative side, it requires a large amount of hardware some of which is specific for each patient and each field. Also there is a dosimetric disadvantage compared to active systems. The reason is that since the high dose region of the SOBP is fixed and only the distal edge is possible to shape (by using the compensator) there is *always* a high dose region between the entrance and the proximal edge of the target. This dose however reduces as several fields are used from different directions. In the case of active systems, they allow for more flexibility in the planning, which will be discussed in next sections. They do not make use of patient specific hardware for the delivery and it also offers a lower production of secondary neutrons in the nozzle. On the negative side, the commissioning as well as the quality assurance tends to be complicated; the flexibility it offers also demands expertise and caution and moving targets are a particular challenge for this type of delivery.

1.1.1 Dose Calculation for active delivery systems

The limited configurations in hardware make the dose calculation in water for passive systems a much simpler problem than for active delivery systems. In his draft paper Gottschalk (12) gives a profound discussion on the dose calculation and design of passive delivery systems.

For active systems the calculation of the absorbed dose is done "spot by spot". That means that the treatment planning system should be able to model the radiation transport of quasi-monoenergetic ion beams inside the patient. Broadly speaking, there are three classes of algorithms that have been suggested and implemented in particle therapy. These are:

Ray Tracing-WEPL :A ray tracing algorithm calculates the dose deposition along the central axis of the path of the particle. To account for the effect of scattering on the dose authors have used an energy dependent gaussian or double gaussian smoothing as in Krämer (15). To account for heterogeneities the concept of

Water-Equivalent-Path-Lenght (WEPL) is used. The WEPL of a material sample is defined as the magnitude of the shift of the Bragg peak after the sample is located in front of the beam as compared to reference measurements.

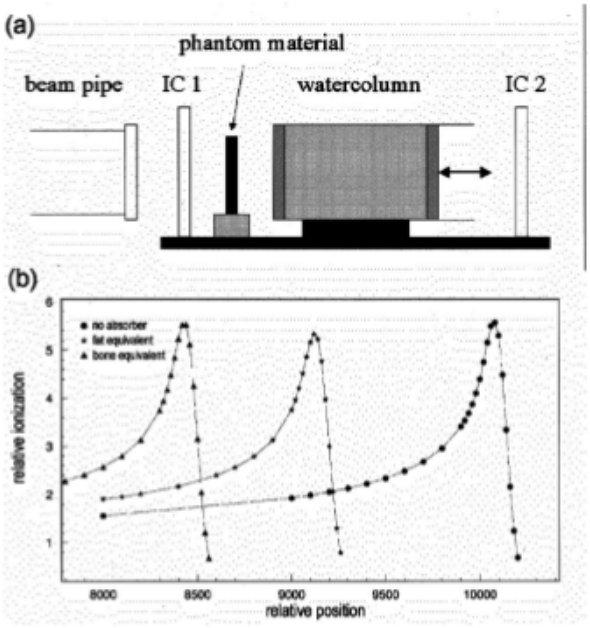

Figure 1.4: WEPL approach for dose calculation 1 - (a) Schematic representation of the experimental set up for WEPL measurements. (b) Depth dose curves obtained by using different absorbers. The shift in the location of the Bragg Peak corresponds to the WEPL value. Taken from (16)

Pencil beam algorithms : Make use of a precalculated dose kernel in water for each of the ion beam energies used in a treatment. These kernels take into account scattering (17). When the dose is calculated in heterogeneous media the dose is scaled according to the stopping power of the material. In that sense only a local correction for scattering is employed. A second generation of pencil beam algorithms was proposed by Szymanowski and Oelfke (18, 19) in which CT data is used to model the non-local aspect of the scattering effect.

Monte Carlo Methods : Considered by many as the gold standard for radiation transport simulations, this methods have been used in nozzle design of passive systems (20, 21). Their clinical implementation in active delivery systems has

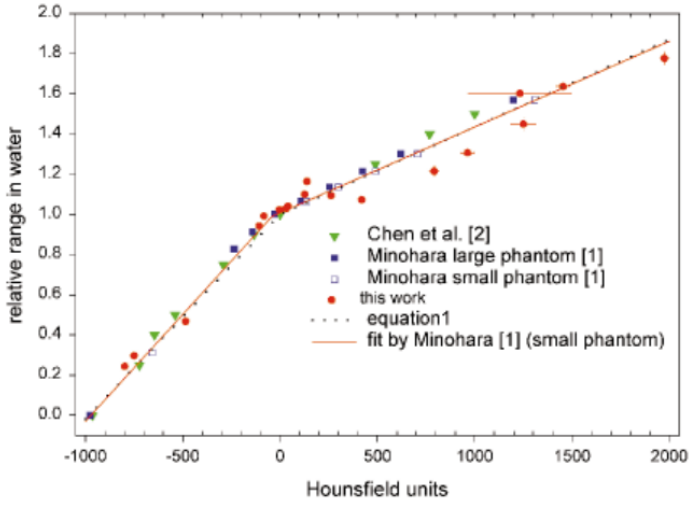

Figure 1.5: WEPL approach for dose calculation 2 - Example of a HU-to-WEPL calibration. Taken from (16)

been reported by Paganetti (22) and Mairani (23). It is expected that as computer performance increases these methods will begin to have a more active role on daily clinical usage.

1.1.2 Active delivery system concepts for treatment planning

Having an active delivery system allows for great flexibility in treatment planning. Various techniques using different complexities of beam spot modulation have been identified and discussed in the literature (24). These are:

Single Field Uniform Dose (SFUD) : With this technique each field delivers a uniform dose to the target by adapting the energy of the particles to conform the proximal and distal edge. It offers an improvement over the dose distribution obtained with passive delivery systems in that all particles stop inside the target volume or within few millimeters from it, as opposed to stopping in healthy tissue located in the proximal region of SOBP.

2.5D Modulation : With this technique the dose is modulated only in the plane transversal to the beam and not in depth.

Distal Edge Tracking (DET) : Proposed by Deasy (25), in this technique the beam spots are located in distal region of the target for each field. The result is that most of the target volume is irradiated with *plateau dose*. The technique delivers perhaps the lowest possible dose to healthy tissue located in the proximal region of the target for each field. A major disadvantage is the location of the highest LET component on the edge of the target close where healthy tissue and organs at risks are often found.

Intensity Modulated Particle Therapy (IMPT) : Although intensity modulation is required in proton therapy to produce even a simple SOBP, the term IMPT refers to use to nonuniform dose distributions from a number of fields that add up to a homogeneous dose distribution(24). In the IMPT technique the intensity of every beam spot becomes a free parameter which has to be set. This is done in a similar way as fluence maps are calculated in the IMRT technique in photon therapy and it is known as inverse planning. Just like in IMRT, constraints to organs at risk can be taken into account. Both SFUD and DET as well as 2.5D modulation can be seen as special instances of the more general IMPT.

Another technique often found in clinical practice is the so called *field-patching*. The technique employs two or more field where each field irradiates uniformly a part of the target. In some cases this helps to reduce medium and high doses in regions close to the target as well as it lowers the integral doses.

1.2 The concept of radiobiological effectiveness in Ion Beam Therapy

Radiation therapy in an empirical discipline. Prescribed doses to the target, to boost regions, tolerance doses and volumes for organs at risk, integral doses, late and acute effects of radiation have all been quantified and studied after more than a century of clinical practice. This clinical practice has been obtained mainly with photon therapy which means that the experience gathered apply for that specific type of radiation quality. However it has been known for decades that absorbed dose does not determine uniquely the effect of radiation in cells and tissue. Not just the quantity of the radiation absorbed but also its quality play an important role in estimating the magnitude of the

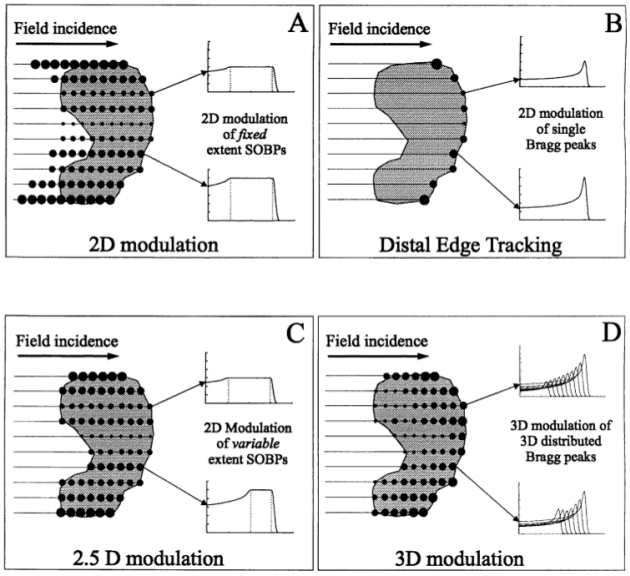

Figure 1.6: The flexibility of the active delivery system - Different techniques available with an active delivery system. (a) Emulation of a passive delivery system (b) Distal Edge Tracking technique, (c) 2.5D modulation, (D) 3-D IMPT technique. Taken from (24)

damage in human cells. When a new radiotherapeutic modality arrives using a different type of radiation quality, questions appear: "Which dose should be prescribed?", "Which effects can be expected in normal tissue?".

Early researchers understood that it was hard to get a quantification of radiation effect in absolute terms for every type of radiation quality. With the years the question was preformulated: "Which dose $D_{applied}$ gives the same effect as D_{ref} Gy of photon dose?"

The concept of radiobiological effectiveness (RBE) was born out of this question. The definition is as follows:

$$RBE = \frac{D_{ref}}{D_{applied}}|_{isoeffect} \tag{1.1}$$

That is, the quotient between the reference absorbed dose (usually obtained with photons) and the dose investigated that give the same issoeffect. In radiotherapy the problem of RBE is the problem of finding the dose prescription for a defined isoeffect.

Mathematically this is often stated as:

$$D_{pres} = RBE * D_{applied} \tag{1.2}$$

The value of the RBE depends among other things on the radiation quality, on the dose, on the specific endpoint under consideration, on the fractionation, on the biological system.

For proton therapy the value of the RBE from cell survival experiments as well as *in vivo* data has been discussed extensively in (26). A generic value of 1.1 is used in almost all institutions independent of dose per fraction, proton energy, location in the target and tissue. To estimate the effects of radiation in proton treatment the absorbed dose is multiplied by 1.1 and the result is given in units of gray equivalent (GyE)[1]. This *RBE-weighted dose* is used to estimate the effect in the tumor and in normal tissue using photon dose response data.

The situation is more complicated for carbon ions since the radiation quality changes dramatically with depth along the depth dose curve. This means that at different locations in target and organs at risk the quantity and the quality of the energy absorbed is different and a generic RBE can not be used. Nowadays only three institutions are treating patients with carbon ions: the HIMAC facility in Chiba, Japan, the HIBMC facility in Gunma, Japan , and the Heidelberg Ion Therapy Center (HIT) in Heidelberg, Germany.

The dose prescription in the Japanese institutions is described in (27) goes as follows:

- For each predefined SOBP, the modulator wheel is designed in such way so that along the SOBP one measures the same effect on a cell survival experiment. The biological system used is Human Salivary Grand (HSG) Tumor cells and the endpoint is 10% survival fraction after irradiation.

- These institutions have had from the past valuable experience with fast neutron therapy. The dose average Linear Energy Transfer (LET) of the fast neutron spectrum used is close to $80\frac{keV}{\mu m}$. HSG cell experiments with mono energetic carbon ions having the same LET resulted on the same issoeffect. Because of this

[1]The unit Gy(RBE) has lately be suggested by the ICRU.

the depth in a SOBP at which the dose average LET is equal $80\frac{keV}{\mu m}$ is referred by them as *neutron equivalent position*.

- The absolute value of the *clinical dose* is obtained by multiplying the absorbed dose at the neutron equivalent position by the clinical RBE known by them from their experience with fast neutron therapy. The value used is $RBE_{clinical} = 3$. The value of the clinical dose is assumed to be constant along the SOBP (thanks to the constant biological dose for the HSG cells endpoint) so the $RBE_{clinical}$ at each depth is calculated by dividing the clinical dose by the absorbed dose at each point along the SOBP.

This prescription is fixed for an specific fractionation schedule and treatment field. Figure 1.7 shows the idea of the calculation.

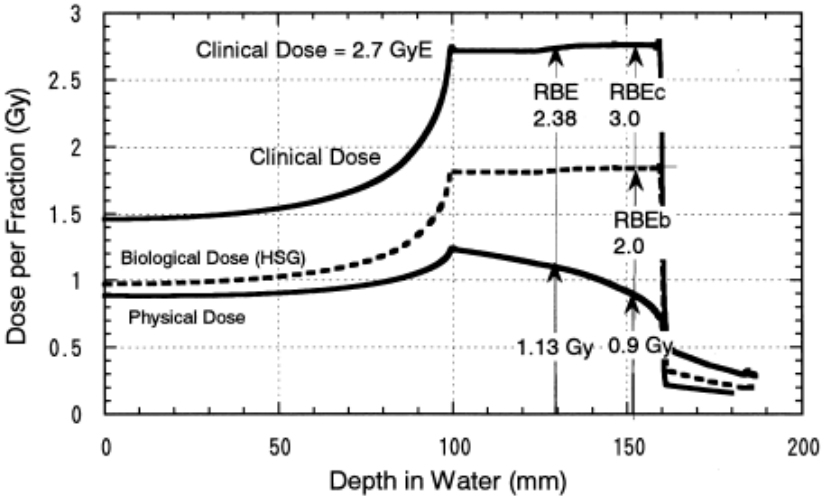

Figure 1.7: RBE concepts at NIRS - The dashed line represents the *biological dose* with an endpoint of 10% survival in HSG cells. The solid line above represents the clinically equivalent SOBP. Taken from (27).

The situation is different at HIT in Heidelberg. Having an active delivery system allows for a very large amount of possible treatment fields each of them with different radiation qualities. Several models have been suggested to estimate the biological effect in ion beam therapy. Hawkins proposed a model based on microdosimetric quantities (29, 30), Wilkens and Oelfke used a phenomenological approach (31) and Scholz and his collaborators proposed the so-called Local Effect Model (LEM)(32, 33). These models

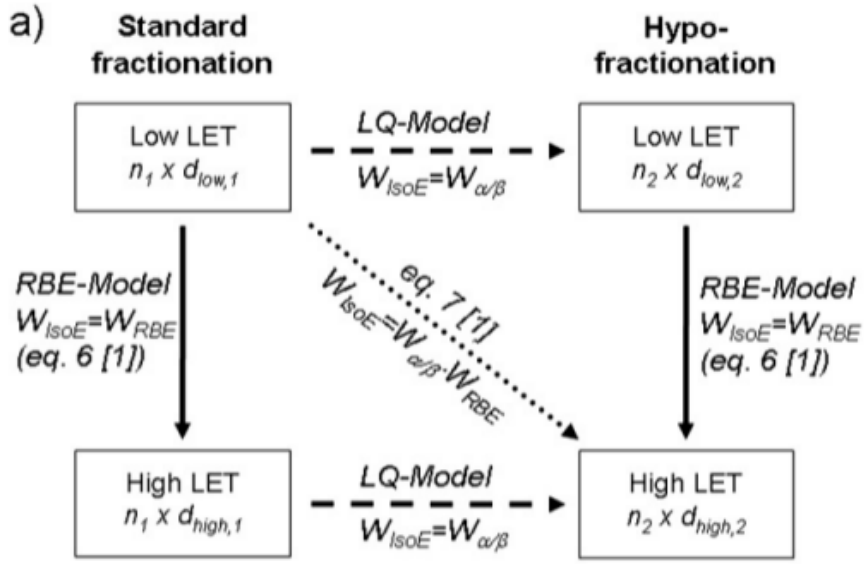

Figure 1.8: From in vitro to in vivo effects - Vertical lines represent the modeling of the biological effect using the LEM model. Horizontal lines represent the step from in vitro to in vivo by means of the Linear Quadratic model. The same approach is used to obtain different fractionation schedules (28).

share in common that (whether by using a functional closed form or a computational procedure) estimate the dependency of α and β parameters of the Linear quadratic model on radiation quality to assess the effect of radiation in *in vitro* experiments. The step from in vitro to *in vivo* assessment of the effect is still an open problem. So far the only model that has been used clinically for an active delivery system is the LEM model. In the LEM model the step from in vitro to in vivo is made via the alpha beta ratio of the biological system in consideration, which is extracted from clinical data. An approach based on the Linear Quadratic model is used. when a fractionation scheme needs to be designed. Figure 1.8 shows this. A comparison between the model and the experimental results was published by Karger (34).

1.3 Inverse planning and optimization

One of the most important developments of modern radiation therapy was Intensity Modulated Radiation Therapy (IMRT). This modality allowed to combine highly modulated photon fields to better conform the dose to the target volumes. It allowed for

conformal avoidance to reduce the absorbed dose in healthy tissue and organs at risk (OAR). In order to fully exploit the potential of the technique and to make use of all the degrees of freedom available a procedure known as *inverse planning* is used (35). Inverse planning uses some of the tools of applied mathematics and specially the one from *optimization theory* to find the fluence maps needed to achieve a certain goal. With the arrival of IMPT these tools where also applied for inverse planning in particle therapy (35, 36).

The description presented below follows Llacer (37) and it shows how the optimization algorithm was implemented in the software used in this thesis.

In order to achieve a homogeneous dose D_{pres} in the PTV Llacer proposed to maximize the function

$$K_2(\vec{w}) = \sum_{i \in PTV} [-\frac{1}{2} ln(2\pi D_i) - \frac{(D_i - D_{pres})^2}{2D_i}] \tag{1.3}$$

using an Expectation Maximization algorithm as done by Shepp and Vardi (38) for the problem of PET image reconstruction. In this formula the vector $\vec{w}$ gives the weight of the modulation of each beam spot. D_i is the dose absorbed in the i^{th} voxel and it depends on $\vec{w}$ but this dependency will not always be stated for the sake of clarity.

By using Picard successive approximations he gets:

$$w_j^{(k+1)} = \frac{w_j^{(k)}}{q_j} \left\{ \sum_{i \in PTV} D_{ij} \frac{D_{pres}}{d_i^{(k)}} \right\} \tag{1.4}$$

where

$$q_j = \sum_{i \in PTV} D_{ij} \tag{1.5}$$

$$d_i^{(k)} = \sum_j D_{ij} w_j^{(k)} \tag{1.6}$$

$w_j^{(k)}$ is the k^{th} iteration of the weight of the j^{th} component of the beam spot modulation vector, $D_i^{(k)}$ is the k^{th} iteration of the value of the dose in the i^{th} voxel and D_{pres} is the prescribed dose.

If one wants to take into consideration dose volume histogram constraint (D_1, V_1) for the OAR the iterative scheme becomes:

$$w_j^{(k+1)} = \frac{w_j^{(k)}}{q_j} \left\{ \sum_{i \in PTV} D_{ij} \frac{D_{pres}}{d_i^{(k)}} + \sum_{l \in M} \beta_l D_{lj} \frac{D_1}{d_l^{(k)}} \right\} \tag{1.7}$$

where

$$q_j = \sum_{i \in PTV} D_{ij} + \sum_{l \in M} D_{lj} \tag{1.8}$$

$$M = \left\{ l \in OAR \mid D_2 \geq d_l^{(k)} \geq D_1 \right\} \tag{1.9}$$

β_l is a penalty factor for the l^{th} voxel of the OAR and D_2 is such that:

$$V_1 = DVH(D_2) \tag{1.10}$$

In the case of a maximal dose constraint $D_1 = D_{max}$ and

$$M = \left\{ l \in OAR \mid d_l^{(k)} \geq D_1 \right\} \tag{1.11}$$

1.3.1 RBE-weigthed dose optimization

For the case of carbon ion treatments is mandatory to take into account the RBE, or in other words, to prescribed RBE-weighted-dose instead of just absorbed dose. The problem is then to find a $\vec{w^*}$ such that:

$$\vec{w^*} = \arg\min_{w} K_1(\vec{w}) \tag{1.12}$$

where

$$K_1(\vec{w}) = \sum_{i \in PTV} (RBE_i(\vec{w})).D_i(\vec{w}) - D_{pres})^2 \tag{1.13}$$

In the previous formula D_{pres} is the prescribed dose in GyE, D_i is the absorbed dose in the i^{th} voxel and RBE_i is the RBE value for that voxel under that specific beam modulation[1].

A problem with this approach is the obvious nonlinearity of the function $RBE(\vec{w})$ which increases the complexity of the optimization problem to be solved. This complexity can translate into extended calculation times which in a clinical environment are undesirable.

[1]Here the endpoint is the one obtained by irradiating the biological system with a D_i with a radiation field having the same quality as the one presented in the voxel

An alternative to the use of the $RBE(\vec{w})$ function is the optimization based on the radiobiological effect. Wilkens and Oelfke(39) proposed a particularly fast approach which will be followed in this work[1].

In the linear quadratic model *the effect* is understood as negative of the logarithm of the survival function:

$$E = -ln(S) = \alpha D + \beta D^2 \tag{1.14}$$

If one thinks of the linear quadratic model as poissonian model for the distribution of lethal lesions, then the effect would be the mean value of lethal lesions as a function of the absorbed dose.

If E_{pres} is the effect obtained after applying a dose D_{pres} and E_i is the effect in the i^{th} voxel, then the problem can be preformulated to the minimization of the function:

$$K_2(\vec{w}) = \sum_{i \in PTV} (E_i(\vec{w}) - E_{pres})^2 \tag{1.15}$$

$$= \sum_{i \in PTV} (\alpha_i(\vec{w}) D_i(\vec{w}) + \beta_i(\vec{w}) D_i^2(\vec{w}) - E_{pres})^2 \tag{1.16}$$

Generally speaking, the quality of the radiation absorbed (often quantified with the LET or by using microdosimetric quantities) changes from voxel to voxel. It has been shown that the value of the alpha parameter increases almost linearly with LET until it reaches a maximum, then decreases. The dependency of beta on LET is still an open problem but it is expected that this dependency is less pronounced as compared to the case of alpha. Zeider and Rossi (40) used the Theory of Dual Radiation Action (41) to estimate the value of the α and β parameters in a mixed field. They proposed to calculate the alpha by doing a dose weighted average of the alpha values obtained with the radiation that makes up the mixed field. This method is also used for the calculation of the square root of beta. Later on Kanai (42) used these relationships in order to estimate the survival of V79 cells irradiated with carbon ion beams. The relationships are the following:

$$\alpha = \frac{\sum_k \alpha_k D_k}{\sum_k D_k} \tag{1.17}$$

[1] This is the approach implemented in PartPlan for RBE-weighted dose calculation.

$$\sqrt{\beta} = \frac{\sum_k \sqrt{\beta_k} D_k}{\sum_k D_k} \tag{1.18}$$

where α_k and β_k are the ones obtained by irradiating the cell lines with the k^{th} component of the radiation field, and D_k is the dose that such component delivered.

In the case of a treatment in a voxelized geometry the alpha value calculated for the i_{th} voxel would be:

$$\alpha_i = \frac{\sum_k \alpha_{ik} D_{ik}}{\sum_k D_{ik}} \tag{1.19}$$

where α_{ik} is the alpha value of the k^{th} beamlet in the i^{th} voxel and D_{ik} is the dose delivered to the i^{th} voxel from the k^{th} beamlet under the given beam modulation. F_{ik} is the dose absorbed in the i^{th} voxel when irradiating the volume with the j^{th} beamspot (or beamlet) with one particle (or one unit of fluence). The dose D_{ik} is equal F_{ik} times the number of particles in the beamspot w_k.

$$\alpha_i D_i = \sum_k \alpha_{ik} F_{ik} w_k \tag{1.20}$$

Setting $\Delta_{ik} = \alpha_{ik} F_{ik}$ we get:

$$\alpha_i D_i = \sum_k \Delta_{ik} w_k \tag{1.21}$$

Similarly for the betas, if we set $\Omega_{ik} = \sqrt{\beta_{ik}} F_{ik}$

$$\beta_i D_i^2 = (\sum_k \Omega_{ik} w_k)^2 \tag{1.22}$$

With this formulas the effect based objective function to minimize becomes:

$$K_2(\vec{w}) = \sum_{i \in PTV} (\sum_k \Delta_{ik} w_k + (\sum_k \Omega_{ik} w_k)^2 - E_{pres})^2 \tag{1.23}$$

Wilkens and Oelfke (39) used a limited memory BFGS algorithm to minimize this function. Another way to solve this problem is to take advantage of the dominant behavior of the linear term in high LET radiation by using a similar iterative scheme as the one shown in the previous section but actualizing the impact of the quadratic term at each iteration. One can think of it as a quasi-linear approach. The method is

very fast and uses a limited amount of memory. The desired beam spot modulation is then:

$$w_j^{(k+1)} = \frac{w_j^{(k)}}{q_j} \left\{ \sum_{i \in PTV} \Delta_{ij} \frac{E_{pres}}{E_i^{(k)}} \right\} \tag{1.24}$$

where

$$q_j = \sum_{i \in PTV} \Delta_{ij} \tag{1.25}$$

and

$$E_i^{(k)} = \sum_j \Delta_{ij} w_j^{(k)} + (\sum_j \Omega_{ij} w_j^{(k)})^2 \tag{1.26}$$

Similar strategies to the ones presented in the previous sections can be used to take into account OAR sparing.

1.4 The challenge of robustness in ion beam treatment plans

Ion beam treatment plans have been known to be very sensible to errors and uncertainties in the modeling and delivering of the dose. Several types of uncertainties might, in some situations, compromise the potential benefits of the modality. Some of these uncertainties are common to all modalities in external radiation therapy like the problem of inter fraction and intra fraction motions. Others are inherent challenges coming from the very laws of the interaction of charged particles with matter raising questions on the precision and accuracy of the dose calculation in a patient. They will be briefly presented below.

1.4.1 Precision and accuracy of the dose calculation

As described above, there is a wide range of approaches for dose calculation in ion beam therapy. Different algorithms use different types of data for modeling the energy deposition in a patient. The precision and accuracy of the dose calculation will generally speaking depend on two things: the uncertainties of the data used (i.e. stopping power values or composition of patient's tissues) and the validity and correctness of the assumptions of the model.

Let's start with the uncertainties of the input data. In a WEPL-based algorithm the accuracy of the calculation is strongly linked to the errors in the Houndsfield Unit-to-WEPL calibration. This calibration is purely phenomenological and is likely to induce a systematic error in the calculation of the WEPL value. As shown in Figure 1.5 there are important deviations from this calibration for PMMA materials and materials with high CT numbers. The calibration also fails to give an accurate value of the WEPL for metal materials due to the obvious problem of obtaining a correct Houndsfield Unit (HU) value for it. For Monte Carlo and pencil beam algorithms, the values of the stopping and scattering powers play the crucial role. The task of accurately estimating the stopping power values in a clinical situation is enormous. Schneider et al (43) proposed a method to calculate the material composition of each voxel based on CT data. One could then used the Bethe-Bloch formula to obtain a value of the stopping power. However one should also take into account that the Bethe-Bloch formula itself might introduce errors. Of particular interest is the so called *I-value* for different materials. It is a matter of intense debate the value of this quantity even for media such as water. These uncertainties lead to an error in the dose estimation at each voxel. Another way of looking at the problem is saying that the uncertainties lead to a *range error*. This interpretation of the problem is often used since it points out the magnitude of the problem under consideration: if particles are not stopping where they are supposed to then the dose absorbed might very heavily deviate, at each point, from the one prescribed.

Even if the data that each of the dose calculation engines take as input has no errors there is the question of the validity of the assumptions used in each model. In Ray-Tracing algorithms scattering of particles is neglected and the effect of such scattering is approximated by using a gaussian or double gaussian smoothing of the dose obtain along the ray. In pencil beam algorithms the dose is laterally scaled according to the value of the stopping powers. As mentioned before, an improvement on this approach was recently proposed (18, 19) where corrections are made to take into account a better description of scattering phenomena. Failing to properly describe the scattering of particles in heterogeneous media leads to dose calculation that could, for instance, neglect the so called *Bragg Peak degradation* phenomenon. Bragg peak degradation is discussed in (44). There is shown that thin inhomogeneities might have strong influence

on the delivered dose usually deviating significantly from what is expected. A graphical representation of this phenomenon is shown in Figure 1.9(b).

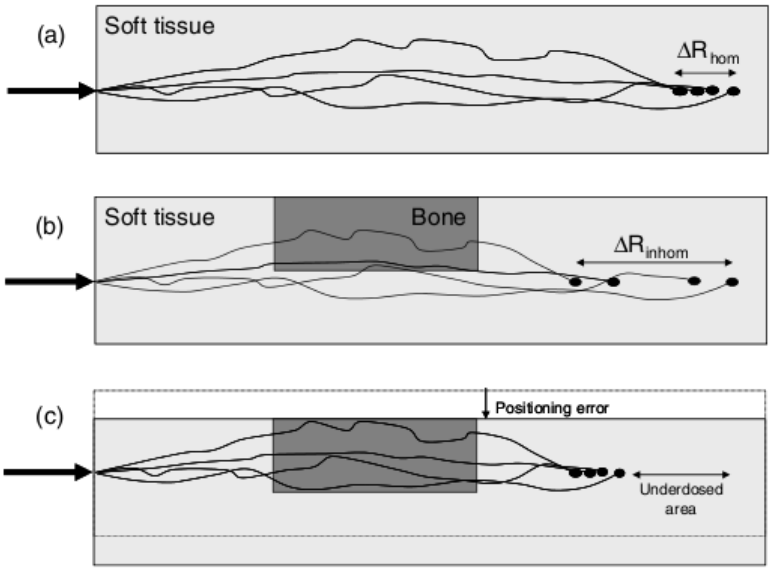

Figure 1.9: Impact of heterogeneities on the range of particles - Figure (b) illustrates the Bragg Peak Degradation. Figure (c) shows the effect of a misspositioning the patient. Taken from (45).

The accuracy of the dose calculation is also connected with the correct modeling of the patient. Being the CT numbers the main parameter for the characterization of the physical properties of the voxel its value must be known with low uncertainties. Lomax (45) has shown that variations of 3% in Houndsfield Units leads to range errors of the order of 5%, that is 5 mm for every 10 cm in water!.

Recently efforts have been put in order to better describe the physical properties of each voxel using alternative imaging modalities. Bazalova (46, 47) used Dual Energy CT to provide a better material segmentation. Hunemohr et al (48, 49) used Dual Energy CT to provide a better HU-to-WEPL calibration.

Another limiting factor in modeling the patient is the resolution of the voxel geometry. Specially in regions of high heterogeneities having a voxel sizes that are too big might lead to an inaccurate assessment of the of the dose calculation failing, for example, to model Bragg Peak degradation.

The problem of the accuracy of the dose calculation and the impact of errors on

the dose delivered remains today, despite significant contributions, an open problem. In clinical practice physicist are encouraged to take special caution when dealing with this type of problems. As Lomax points out:

> "Our analysis seems to imply, of these two problems, range uncertainty is the most important, as it has a potentially larger effect on the dose distribution than uncertainty in the dose calculation. However, as the effects of both uncertainties could very well be systematic over all fractions, we would advise that particularly complex plans are routinely analyzed taking such effects into account."(45)

1.4.2 Intra- and Inter-fraction motions

For interfraction motions we will understand the type of errors induced by the inaccurate assessment of the position of the relevant structures from fraction to fraction. The source of these errors can be either a modification in the patient's anatomy, a movement of the relevant structures with respect to an internal frame of reference or a misspositioning of the patient in the treatment table. The later will be also referred as set-up (SU) error.

To avoid set up errors is a task that every medical physicist working in the clinic has to face independent of the modality of external radiation therapy. With the arrival of Image Guided Radiation Therapy (IGRT) tools have been found to address this problem, or at least, to fully known its extension. The situation is potentially more dangerous in ion beam therapy than in photon therapy since a misspositioning of just few millimeters might lead to the incorrect placement of beam spots. This situation is shown in Figure 1.9(c).

The impact of set up errors on ion beam plans has been studied by Lomax (50) in the case of proton therapy and Karger et al (51) for Carbon Ion Therapy. Karger analyzed the effect of set up errors on plans of cervical spine tumors for both IMRT and carbon ion therapy with an active delivery system. He concluded that carbon ion therapy is more sensible to set-up errors that IMRT. For the particular case of cervical spine tumors he observed a larger deviation for carbon ion therapy in the dose measured in the organ at risk as compared to IMRT.

Lomax on the other hand has shown the importance of imaging prior to dose delivery for each fraction. He showed that although misspositioning errors can correspond to histograms with arbitrary shapes, if one repositions the patient using IGRT based imaging techniques the residual error in the position can be well approximated by a bell shaped probability density function (in each of the three dimensions) having an average value of zero and a standard deviation below 1.5 mm. That is probably as good as it gets for dealing with this kind of uncertainties. They cannot be fully eliminated from the treatments and one could only hope to reduced them to a minimal expression, characterize them and take countermeasures to compensate for the impact they might have in the treatment.

Intrafraction motions will be understood as the movements occurred during the delivery of the dose. This problem is often known as the *organ motion problem*. The problem of organ motion has been studied by Bert (52, 53, 54), Furukawa (55) and Kraus (56) in the context of ion beam therapy with active delivery systems. The interference of the scanning pattern and the motion of the organ produces a dose distribution that is, usually, heavily deteriorated and its known as *interplay effect* The problem is more severe as the number of fractions decreases.

In order to reduce interplay effect, three mitigation techniques have been proposed: rescanning, gating and tracking. In the rescanning technique the delivery of the dose in each beam spot is not done at once but it is divided into several instances. The idea behind is that organ motion will have a different effect in each instance averaging out the dose delivered to each spot. Gating is a technique used in other types of external radiation therapy. The idea behind gating is to a priori characterize the movement of the organ and deliver the dose in the time phase in which the movement is minimal. It often assumes that the organ moves in constant, periodic motion. Finally, tracking aims to take into account the movement of the target and "paint it as it moves". In involves fast adaptation of the treatment parameters as the organ moves.

The potential use in clinical practice of these mitigations strategies is being investigated and studied (52, 53, 54, 55, 56) as right now this is one of the aspects limiting the applicability of the active delivery system.

2

The problem of PTV definition in Ion Beam Therapy

"In addition, for proton therapy using spot scanning, as performed at our institute, collimation and compensation are not used, meaning that the traditional methods of dealing with uncertainties cannot be adopted. For this reason, we nevertheless currently manage delivery uncertainties using the PTV concept as in conventional therapy."(50)

Prof. Dr. Wolfgang Schlegel from the German Cancer Research Center (DKFZ) and the University of Heidelberg usually refers to radiation therapy as the art of hitting a target we do not see with an invisible beam. The sentence, simple and rhetorical, embraces one of the fundamental challenges of dose delivery in radiation oncology. As discussed in Chapter 1, several sources of errors have made the problem of dose delivery difficult. Some of these are: the motion of the tumor due to physiological processes, the miss-positioning of the patient prior to delivery, the movements of the patient during the treatment, the changes in the tumor volume and shape as well as the changes in the anatomy of the patient as a result of the treatment.

Clinicians early realized that something was needed in order to take care of the effects of errors and uncertainties present in the delivery of radiation. The first step was, obviously, to try to minimize the value of these errors. This led to the development of immobilization devices, treatment simulators and positioning systems which can be found in hospitals today. The second step established a framework that aimed

to guarantee the correct dose delivery in the presence of (the previously minimized) uncertainties. The idea was to make sure that the dose delivered to the tumor deviates only slightly from what is prescribed. It was an issue of *robustness*. In the heart of this framework lay the concepts of Target Volumes. In the next sections these concepts will be explained as they are proposed in the ICRU 50, 60 and 78 (57, 58, 59) and later in the chapter it will be shown how they are inappropriate for Ion Beam Therapy. Then *Dynamic Target Definition* will be introduced as a way to update the concept of Target Definition for proton and ion beam therapy.

2.1 Target Volume Definitions

2.1.1 Gross Tumor Volume

The Gross Tumor Volume (GTV) is the macroscopic malignant mass that can be identified by the use of different imaging techniques. Its determination and size depends mainly on two factors: the imaging modalities used and the subjective experience of the clinician. X-rays were often used in the past for such determination. With the development of new types of imaging it is now possible to use transmission computer tomography (CT), positron emission tomography (PET), single particle emission tomography (SPECT), nuclear magnetic resonance (MRI) and ultrasound. Having different imaging modalities makes it possible to have quantitative information of the anatomy and physiological processes in a given region of the patient allowing to make a clearer distinction between what is malignant and what is not.

2.1.2 Clinical Target Volume

Since all imaging modalities have limited resolution there will always be malignant cells that will not be identified as a part of the GTV. The Clinical Target Volume (CTV) is the expansion of the GTV that aims to include those tumor cells. *It is the fundamental volume, the clinical statement of what is needed to be treated.* Its determination occurs *prior* to the selection of treatment modality or technique used.
The CTV is usually created by expanding the GTV by margin. Depending on the type of tumor and its location the size of the margin will be different. Clinical experience based on the history of local recurrence for patients with the same type of tumor plays a fundamental role.

2.1.3 Internal Target Volume

The Internal Target Volume (ITV) is an expansion of the CTV by a so-called Internal Margin (IM). The value of this margin is given by the variations in shape, size and position of the CTV with respect to an internal frame of reference. The main motivation for this structure is to take into account the changes in the position and the shape of the CTV due to anatomical changes in the patient during the course of a treatment or during the course of a fraction. A good example is the motion of the CTV in lung cancer patient due to breathing. The concept was introduced in the ICRU 62 (58) in a moment when IGRT was *ad portas* of worldwide clinical implementation.

2.1.4 Planning Target Volume

Each treatment modality has intrinsic inaccuracies and errors that challenge the delivery of the dose to the CTV. The Planning Target Volume (PTV) is an expansion of the ITV (or the CTV, if the ITV is neglected) that aims to take into account all the net effects of all the geometrical variations and inaccuracies so that the CTV receives the prescribed dose. Some examples of the kind of errors that the PTV concept aims to mitigate are:

- the miss-positioning of the patient in the treatment room prior to delivery.
- mechanical uncertainties of the equipment
- dosimetric uncertainties

It is worth mentioning that the size of the beam has to adjusted so that the width of the penumbra falls outside of the PTV. The size of the PTV volume is then a geometric construction dependent on the degree of uncertainties *of a specific modality and delivery technique in a given institution.*

Although the idea of volume expansions might be straightforward to understand, the size of the margins itself is not trivial and it is a topic on intense debate in the literature (60, 61, 62). Figure 2.2 shows different margin recipes taken from different authors.

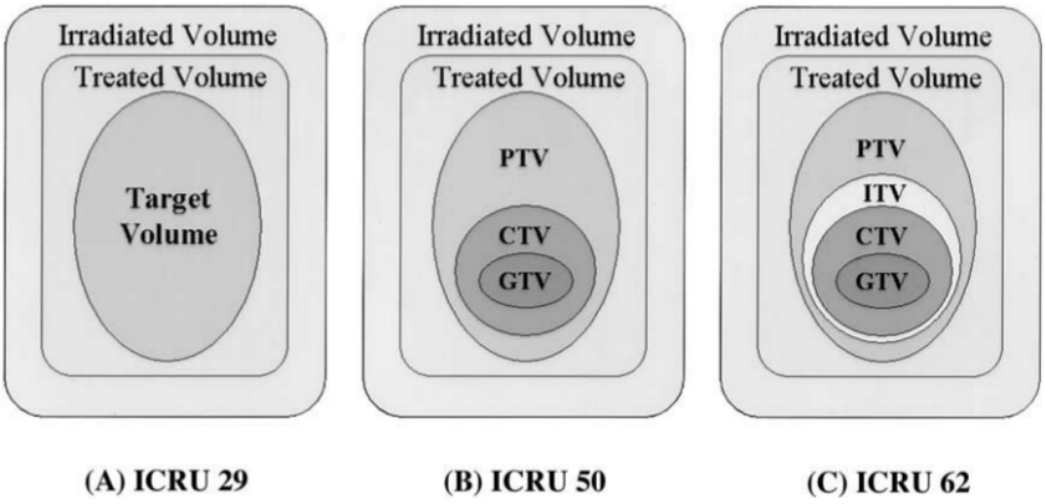

Figure 2.1: Volume concepts in Radiation Therapy - taken from (62)

2.1.5 Additional Volumes

Other structures are defined in the ICRU 50 and 62(57, 58), some of which are important for the discussion in the next sections. They are:

The Treated Volume (TV): The volume receiving a dose equal or larger than 95% of the prescribed dose.

The Irradiated Volume: The volume of tissue receiving a dose that is significant compared to the tolerance of the normal tissue.

The Organs at Risk (OAR): Organs or volumes of tissue whose function might be affected given their intrinsic radio-sensitivity.

The Planning Organs at Risk Volumes (PRV): An expansion of the OAR by an internal margin and a set-up margin. It is an analogous expansion as the one done from the CTV to the PTV. The idea behind the PRV is to make sure that the dose absorbed in OAR are below the threshold, even in the presence of uncertainties.

The volumes described above are shown in Figure 2.1.

Table 2. Summary of Published Margin Recipes for Target, Respiration (Target) and Organs of Risk

Author	*Application*	*Recipe*	*Assumptions*
Bel et al, 1996b[59]	Target	$0.7\ \sigma$	Random errors only (linear approximation) Monte Carlo
Antolak and Rosen, 1999[81]	Target	$1.65\ \sigma$	Random errors only, block margin?
Stroom et al, 1999[51]	Target	$2\ \Sigma + 0.7\ \sigma$	95% dose to on average 99% of CTV tested in realistic plans
Van Herk et al, 2000[43]	Target	$2.5\ \Sigma + 0.7\ \sigma$ or (more correct): $2.5\ \Sigma + 1.64\ (\sigma - \sigma_p)$	Minimum dose to CTV is 95% for 90% of patients. Analytical solution for perfect conformation
McKenzie et al, 2000[60]	Target	$2.5\ \Sigma + \beta\ (\sigma - \sigma_p)$	Extension of van Herk et al for fringe dose due to limited number of beams
Parker et al, 2002[82]	Target	$\Sigma + \sqrt{(\sigma^2 + \Sigma^2)}$	95% minimum dose and 100% dose for 95% of volume. Probability levels not specified
Van Herk et al, 2002[52]	Target	$2.5\ \Sigma + 0.7\ \sigma - 3$ mm or (more correct): $\sqrt{2.7^2\ \Sigma^2 + 1.6^2\ \sigma^2} - 2.8$ mm	Monte Carlo based test of 1% TCP loss due to geometrical errors for prostate patients
Van Herk et al, 2003[69]	Target	M − 2 mm M − 5 mm	Correction for nonuniform cell density
Ten Haken et al, 1997[83] and Engelsman et al, 2001[84]	Respiration (liver and lung)	0 A	No margin for respiration but compensation by dose escalation to iso-NTCP, reducing target dose homogeneity constraints
McKenzie et al 2000[50]	Respiration	A	Margin for respiration on top of other margins when respiration dominates other errors
van Herk et al, 2003[47]	Respiration (lung)	0.25 A (caudally) 0.45 A (cranially)	Margin for (random) respiration combined with 3 mm random SD, when respiration dominates other errors (A > 1 cm)
McKenzie et al, 2002[85]	OAR	$1.3\ \Sigma +/- 0.5\ \sigma$	Margins for small and/or serial organs at risk in low (+) or high (−) dose region

Abbreviations: Σ, SD of systematic errors; σ, SD of random errors; σ_p, describes width of beam penumbra fitted to a Gauss function; A, peak-peak amplitude of respiration; M, margin before adjustment for described effect.

Figure 2.2: Brief summary of Margin Recipes - taken from (61)

2.1.6 Conformal Avoidance and Conformity Index

During the last two decades of the 20^{th} century radiotherapy lived a technological revolution. The incorporation of computers in clinical practice brought not only the advances in imaging and information management to the radiation therapy departments but also, together with invention of the Multileaf collimator (MLC), gave rise to the automatization of the so-called 3-D Conformal Radiation Therapy (3DCRT) and later the well known Intensity Modulated Radiation Therapy (IMRT). These two techniques of conformal radiation therapy allow to spare the normal tissue and OARs reducing the severity of complications associated with radiation therapy. This is know as *conformal avoidance* and it was the main motivation for the development of this type of technique.

It has been stated that a homogeneous dose distribution to the PTV is desirable (57, 58). Since this requirement is in practice very difficult to achieve the ICRU 62 (58) recommends not to allow the deviations of the values of the dose fall below 95% or go beyond 107% of the prescribed dose. The same report introduces a measure of conformity called the *conformity index* (CI) defined as the size of the treated volume divided by the size of the PTV:

$$CI = \frac{\text{Size of the TV}}{\text{Size of the PTV}} \geq 1 \text{ while PTV} \subseteq \text{TV} \tag{2.1}$$

Following the recommendations, the value of CI should be as close to one as the technique allows it to be.

2.1.7 Static Dose Cloud Approximation

If one tries to deal with uncertainties by using volumes expansions like the one made from CTV to PTV a subtle assumption is being made. The dose distribution is then treated as a rigid three dimensional object whose values are not affected by these uncertainties, but only its position in a external frame of reference. The idea is that if the PTV is large enough, the CTV would *swim* in a pool of therapeutic dose. This assumption is sometimes referred as the *Static Dose Cloud Approximation* (63). In principle the assumption is incorrect. It has been reported (64, 65) that for photon therapy changes in the dose values up to 5% can been seen in the dose distribution. There are reasons however why to hold on this assumption. First, the assessment of the impact of uncertainties on detailed radiation transport in a patient is by no means

trivial. In fact, it can be regarded as an open problem. Second, if the variation of the dose in each voxel is no higher than 5% then the error introduced in the approximation is in the order of magnitude of the error in the measurement of the dose in water. The approximation seems then reasonable, for photon therapy.

2.2 The problem of PTV definition in Ion Beam Therapy

As discussed above, the main assumption holding the PTV concept is the validity of the static dose cloud approximation and the isotropic impact of uncertainties on the delivered dose. For Proton and Ion Beam therapy to benefit from these concepts one has to make sure that the mentioned assumptions are still valid for this type of therapy.

As a starting point let's see if, in general, the static dose cloud approximation seems reasonable. Figure 2.3 shows the ideal locations of beam spots for a simulated treatment of proton therapy with an active delivery system. In this case the beam is being delivered through the nose. The green volume can be regarded as the PTV and the red volume represents an OAR. Now lets assume that a small misalignment of 2 mm in the left-right direction is made while positioning the patient. Figure 2.4 shows the locations of the beam spot under the unwanted miss-positioning[1]. Once can see that distortion in the configuration of the beam spots arrangement is enormous. The magnitude of the displacements is not the same for all beams spots, neither its direction. It is not difficult to conclude that the overall distortion of the dose distribution is by more complex than just a "three dimensional shift".

In clinical practice beam arrangements that go through regions of complex heterogeneities are usually avoided. The previous example shows that a small error in miss-positioning can have a serious effect on the location of the beam spots. Another reason to avoid lateral interfaces is the challenge that they brings to the accuracy of the dose calculation. As mentioned in Chapter 1, most algorithms used for dose calculation make simplifying assumptions on the transport of particles and its derived quantities, like the absorbed dose. Often used algorithms, like *ray tracing algorithms* or simplified *pencil beam algorithms* are inaccurate in these kind of conditions.

Whether the beam angle makes the treatment extremely sensible to set up errors

[1]These are calculated using a ray tracing-WEPL approach. The estimation of the location of the beam spots depends on the type of dose calculation used

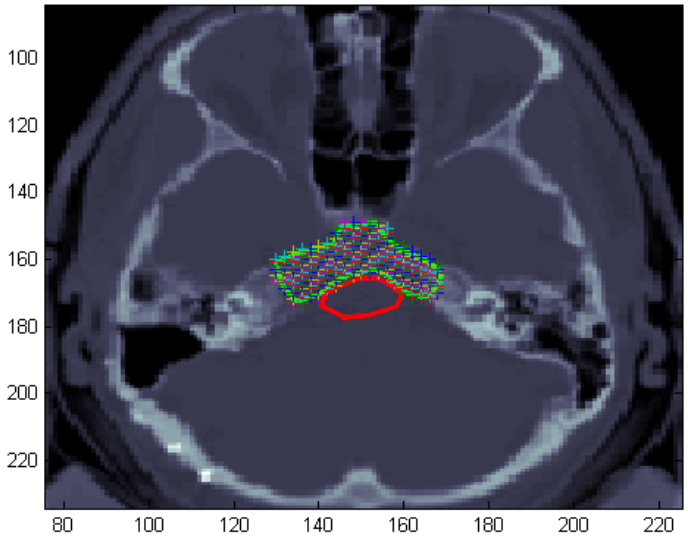

Figure 2.3: Assumed beam spot locations - Contour in green represents the PTV the and in red an OAR. Arrows are beam spot locations.

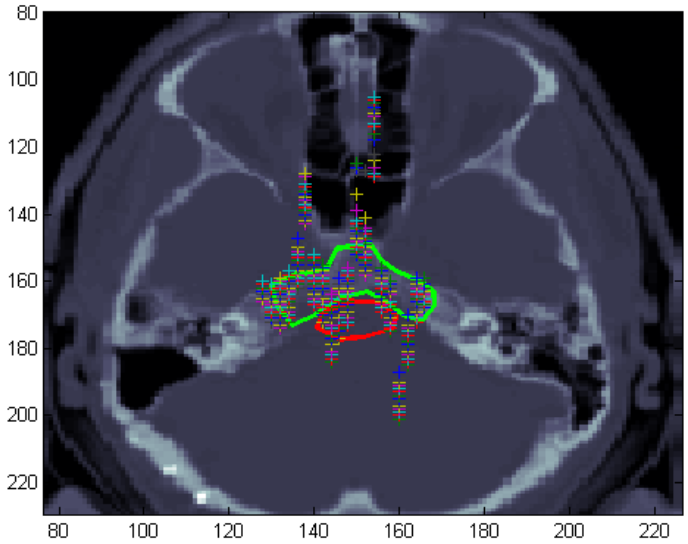

Figure 2.4: Beam spot location after an error in positioning of 2 mm - Contour in green represents the PTV the and in red an OAR. Arrows are beam spot locations.

or whether the accuracy of the dose engine is challenged by complex heterogeneous geometries, a volume expansion does not help to mitigate the effect of these uncertainties. The reason is simple: the static dose cloud approximation, in general, does not hold in particle therapy.

The isotropic impact of uncertainties on the delivered dose is also challenged in particle therapy. The reason is that there is an additional source of uncertainty in this type of modality: the value of the stopping powers (SP) or its related quantity, the Water Equivalent Path Length (WEPL) of the materials inside the patient. This uncertainty translates into an uncertainty in the range of the particles. To illustrate the problem consider the following example:
Figure 2.5 shows a cylindrical phantom consisting of three materials: an outter ring made out of bone tissue, an inner ring made out of lung tissue and an spherical tumor made of water equivalent materials.

Structure	Material	Relative WEPL	WEPL Uncertainty
Outter ring	Bone tissue	1.6	10%
Inner ring	Lung tissue	0.3	20%
Spherical tumor	Water equivalent tissue	1	5%

Table 2.1: Relative WEPL and uncertainties of materials in Figure 2.5.

Table 2.1 shows the values of the WEPL relative to water used for this example. Let's also assume that we have assessed the relative uncertainty of this values and that they are as shown in Table 2.1. These values are not necessarily the ones used in clinical practice and the uncertainties shown reflect in a pessimistic way a worst case scenario useful for this discussion. What is important to consider is that:

- The uncertainty of different types of tissue is in general, different.
- Tissues that are close to water equivalence show a reduced uncertainty often lower than 5%.
- The accuracy of the assessment of the WEPL is reduced for materials with large or very low values of Houndsfield Units (HU).

Let's also assume that there is one and only one source of uncertainty to consider: the WEPL values. In this idealized case no other type of uncertainty will have an effect.

Figure 2.5 shows the isodoses for a one beam proton plan using a SFUD technique. A constant RBE of 1.1 will be used here.

Notice that in Figure 2.5 the PTV is the exact same volume as the CTV. That would be appropriate if no uncertainties were needed to be taken into account. How will the lack of a margin affect the robustness of the treatment towards CTV dose coverage? In order to answer this question let's proceed in the following way:

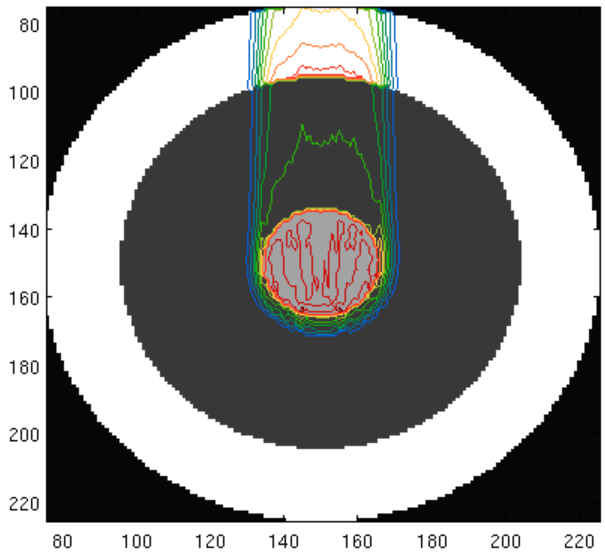

Figure 2.5: Idealized case for the study of stopping power uncertainties - 100% isodoses shown in red, 90% isodoses shown in orange, 40% isodoses shown in green and 10% isodoses shown in blue.

1. Calculate the energies and beam spot weights necessary to achieve a homogeneous dose delivery in the CTV. This is the nominal plan. Store these values.

2. Following a bayesian approach represent the uncertainty of the WEPL values using a probability density function (pdf).

3. For each material, sample a new instance of the WEPL values from the pdf's obtained in the previous step and assign these WEPL values to the materials of the phantom. In other words: create a new instance of the patient.

4. Perform a forward calculation using the energies and weights calculated in step 1. Store the resulting dose distribution.

5. Go to step 3 and repeat until a predefined number of dose distributions N_{max} has been collected.

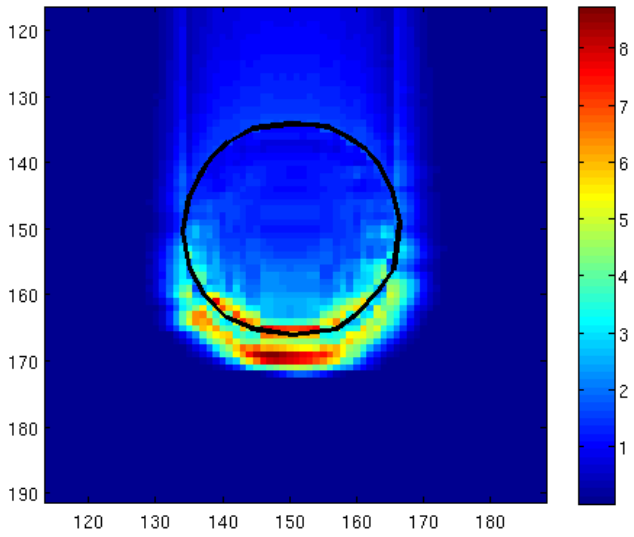

Figure 2.6: Uncertainty of the dose calculation - Standard deviation of the dose values for each voxel in percent of prescribed dose.

For each voxel we have now a histogram of $N_{\max}$ realizations of dose values. The uncertainties of the WEPL have propagated into an uncertainty on the dose for each voxel. If the uncertainty of the WEPL has an impact of dose coverage on the CTV one should be able to find voxels having a histogram that

- have a large dispersion of dose values and/or
- have an average value that differs significantly from the prescribed dose.

Those voxels that result *unaffected* by uncertainties will be refereed as *safely treated*. Figure 2.7 shows in red those voxels which are safely treated. The black contour is the CTV. The following considerations were taken while calculating them:

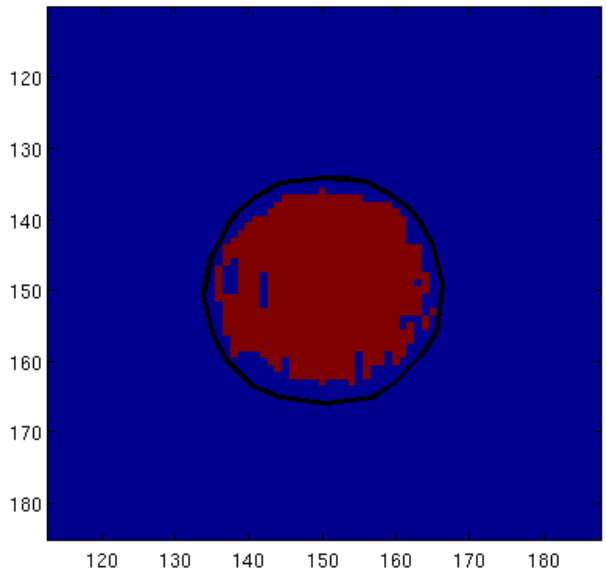

Figure 2.7: Impact of the WEPL uncertainties in CTV coverage - Red voxels are considered safely treated; the black line determines the CTV

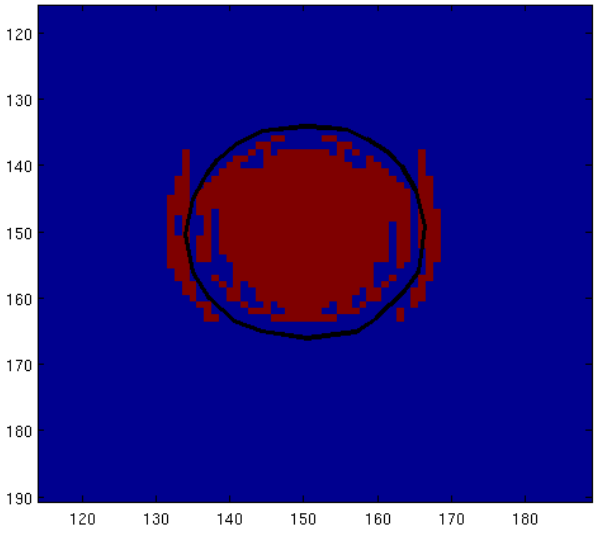

Figure 2.8: Impact of the WEPL uncertainties in CTV coverage after applying a margin - Red voxels are considered safely treated; the black line determines the CTV; the volume treated was an expansion of 5 mm.

- As a measure of dispersion, the standard deviation was calculated. A voxel having a histogram with a dispersion larger that 3% was not considered to be safely treated.

- A voxel having a histogram with an average value deviating by more of 5% from the prescribed dose was not considered to be safely treated.

- The WEPL values were sample from rectangular (uniform) probability density functions having a variance according with the uncertainty values given in Table 2.1.

- A number of $N_{max} = 100$ samples were done.

In Figure 2.7 can be seen that, in fact, some of the voxels of the CTV are not safely treated. Not surprisingly, those voxels located in the distal part of the beam resulted more affected by the range uncertainty than those in the lateral part of the beam. Figure 2.6 shows the values of the standard deviation of the histograms for each voxel. Figure 2.8 shows the result of the procedure of histogram generation and uncertainty propagation to a PTV that is a 5 mm expansion of the CTV. We can see that the problem of *robust dose coverage* is not solve by applying a 5 mm margin. This concern is well expressed by Gotein:

> "Protons require margins in depth to take range uncertainties into account, as well as the more traditional lateral uncertainties. At present, these margins are often quite substantial, especially in the lung whose low density results in the physical extent of the depth overshoot being some four to five times greater than would be the case in, say, muscle. *A combination of technical, imaging, and procedural advances need to be developed to reduce this problem to an acceptable level*" (66)

We can then state that for Ion Beam Therapy:

- In general terms, the static dose cloud approximation does not hold.

- The impact of uncertainties (specially those that propagate into range uncertainties) is non-isotropic.

- Any expansion should take into account beam arrangements and probably beam spot modulations.
- Adding arbitrarily margins by using margin recipes as way to deal with uncertainties can lead to PTVs that are extremely large.

2.3 Dynamic Target Definition in Ion Beam Therapy

As it was mentioned in the previous section the PTV in Ion Beam Therapy is often obtained by adding distal and non-distal (lateral and proximal) margins. The value of the distal margins is calculated on the basis of the range uncertainty (59). However the range uncertainty, as well as any other type of uncertainty, is important to be taken into account simply because it has the property of being able to *propagate into an uncertainty in the dose delivered*[1]. The value of the margin should not be dictated by the range uncertainty (nor the set-up uncertainty or the tumor motion) but by the value of the dose uncertainty. Any useful margin recipe should minimize the dose uncertainty in the CTV while keeping the Treated Volume as small as possible.

Looking at Figure 2.7 one can see that set of voxels safely treated make and almost compact subset of the CTV. The reason why (for this case) the subset is not entirely compact is that some of these voxels miss at least one of the conditions to be considered safely treated. However it is important to realize that the values of the standard deviations and the fluctuation for the mean have an inherent uncertainty depending on how large is the population of the histogram. To avoid this " statistical artifact" one can either increase the number of dose calculations and/or one could apply a *smoothing operation* to the set of voxels safely treated. The important thing to notice is the existence of a quasi-compact subvolume of voxels safely treated.

Having this in mind let's build on some of the concepts introduced on the previous section. Let's define:

tCTV(m,v) : The compact subvolume of CTV voxels that are *safely treated*, under the assumption that a voxel is safely treated if the standard deviation of the histogram generated is lower than v and the average value of the histogram generated differs

[1] In general to an uncertainty in the delivered RBE-weighted-dose

from the prescribed dose by at most m. Both values given in percentage of the prescribed dose.

PTV(m,v) : The compact volume to which the prescribed dose is planned and delivered. The relation between tCTV(m,v) and PTV(m,v) is such that the tCTV(m,v) is the compactification of the CTV voxels that were safely treated when the prescribed dose was plan on PTV(m,v).

The task is now to find the PTV such that for given values m and v,

$$tCTV(m,v) = CTV \tag{2.2}$$

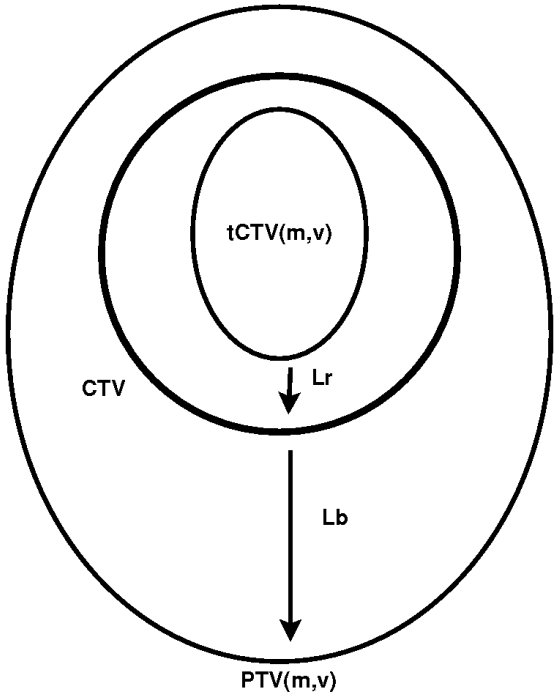

Figure 2.9: PTV(m,v) construction - Relevant volumes for the construction of the proposed CTV expansion

To find such PTV we propose an iterative construction of the volume:

1. Denote L_r the distance from a point of the tCTV to the CTV in the direction normal to the tCTV surface.

2. Along that direction move a distance L_b from the border of the CTV. If the point of the tCTV is outside the CTV then move in the anti-parallel direction (towards the CTV). L_b will be calculated from the relationship:

$$\frac{L_b}{L_r} = \frac{\text{average WEPL of the CTV}}{\text{average WEPL outside the CTV}} \tag{2.3}$$

where by 'outside' is meant the close surroundings of the CTV in the direction of L_b.

3. The point reached is a point of the contour of the PTV(m,v).

4. Plan for uniform coverage of the obtained PTV(m,v). Using this volume, create a new dose histogram and assess a new tCTV(m,v).

5. Iterate until tCTV(m,v)=CTV.

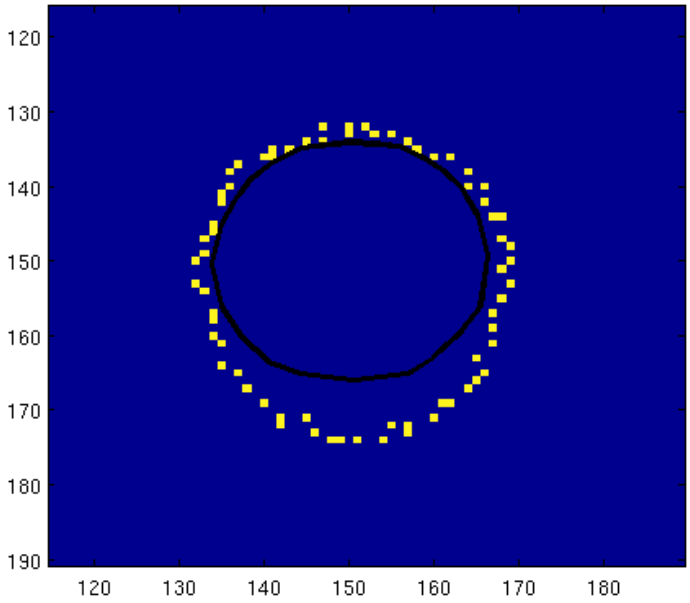

Figure 2.10: PTV(m=5%,v=3%) - PTV derived using the proposed approach for the case shown in Figure 2.5

Figure 2.10 shows the obtained PTV(m=5%, v=3%) after two iterations. Figures 2.11 and 2.12 show the tCVTs after one and two iterations respectively.

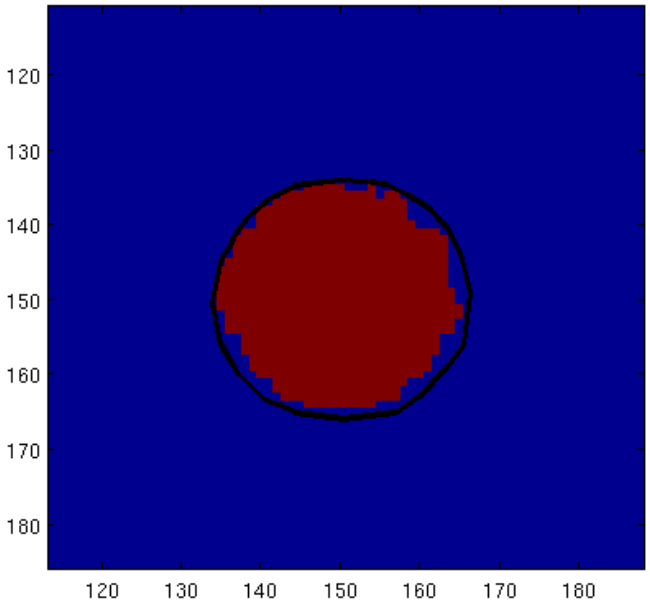

Figure 2.11: tCTV(m=5%, v=3%) - First iteration for the case shown in Figure 2.5

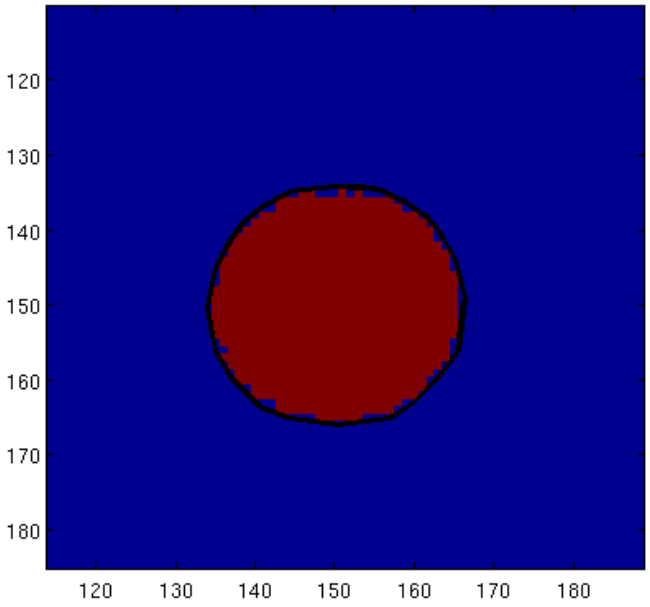

Figure 2.12: tCTV(m=5%, v=3% - Second iteration for the case shown in Figure 2.5

The volume generated (Figure 2.10) is smaller than the isotropic 5 mm expansion (Figure 2.8). This fact can be seen in the Dose Volume Histogram (DVH) shown in Figure 2.13, where the dose in the respective PTVs and the integral doses are plotted. It can also be seen in Figures 2.11 and 2.12 that dose coverage in the CTV (in the presence of uncertainty) has been improved as compared to Figure 2.8.

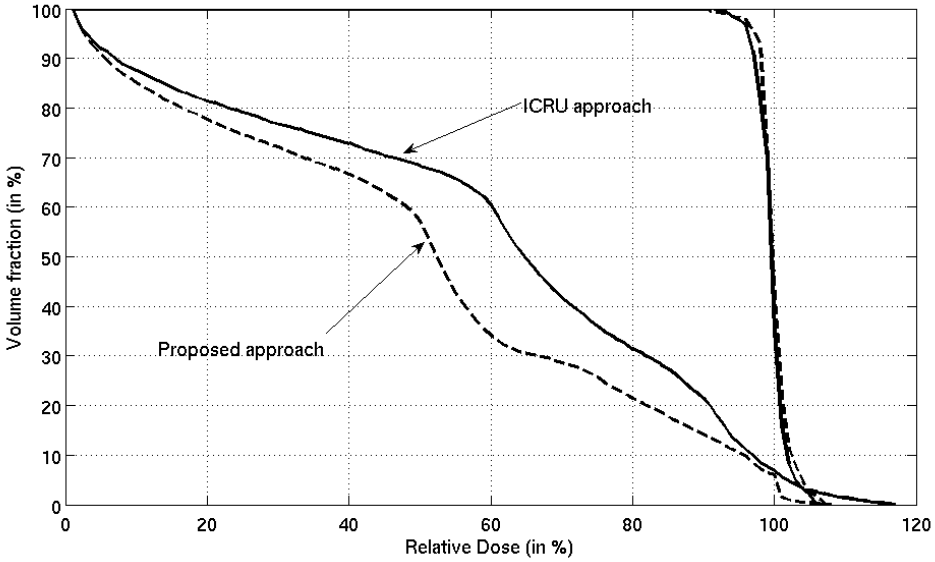

Figure 2.13: PTV and Integral doses - Solid lines represent the 5 mm isotropic margin expansion scenario. Dashed lines represent are for the volumes obtained with proposed method. Although the PTV coverage seems to be adequate for both expansions Figure 2.8 and 2.12 show how different the mitigation of the error really is.

2.3.1 A Head and Neck case

The results of the previous section motivated the application of the method to a two dimensional Head and Neck (H&N) case. To make the study more faithful to the situation found in clinical practice let's not only take into account the range uncertainty coming from an inaccurate assessment of the WEPL values but also let's take into account the uncertainty introduced by (miss)positioning the patient in a fractionated treatment. A single field uniform dose technique (SFUD) was used.

The estimation of the WEPL values will be done using a HU-to-WEPL calibration taken from (16). The quantification of the uncertainty of the WEPL value will be done

in the following way:

- Voxels having a HU value lower than -300 will be assigned a relative uncertainty of 20%.
- Voxels having a HU value higher than 700 will be assigned a relative uncertainty of 10%.
- For the remaining voxels a relative uncertainty of 5% will be assigned.

It is up to the user of the methodology described here to set the values of the WEPL uncertainties[1].

The values used here might seem large but is worth noticing that by using a large uncertainty we are taking a worst case scenario approach and by doing so, we are putting ourselves on the safe side [2]. Also it is important to remember that even if the HU-to-WEPL calibration results in a perfect fit with a theoretically established background there would still be an error induced by treating different tissues as having the exact same composition (water equivalent). It is then evident than in the assessment of the absorbed dose using a HU-to-WEPL calibration a number of random and systematic errors are being induced[3]. The quantification of these errors by a probability density function is the heart of the *bayesian approach* taken here.

For the miss-positioning errors in a multifractionated treatment of proton therapy Lomax (67) shows that by using alignment techniques common in IGRT they are well described by a bell shaped probability density function centered around zero. For this case two zero centered gaussian functions will be used to model the offset of the patient: One with a $\sigma = 2$ **mm** in the Left-Right (LR) direction and another one with $\sigma = 1$ **mm** in the Anterior-Posterior (AP) direction. This choice is arbitrary. In clinical practice the values of these uncertainties should be assessed by the medical physicist.

Inspired in the previous section the uncertainty propagation is performed by doing:

1. Calculation of the nominal plan: Calculate the energies and beam spot weights necessary to achieve a homogeneous dose delivery in the PTV[4]. Store these val-

[1] If the dose calculation algorithm uses the stopping power of the material instead of the WEPL, then an uncertainty should be assigned to it.

[2] In an informal way we could say that we are applying a margin *to the uncertainty* rather than to the volume. Only in extreme cases, the use of very large uncertainties might lead to very larges PTVs.

[3] The calibration used here is purely phenomenological

[4] For both beams simultaneously.

ues. In the first dose histogram creation any initial guess for the PTV can be used. Here $PTV = CTV$ was used[1].

2a. Representation of uncertainties: Represent all the uncertainties to be taken into account with probability density functions. In this case they will be: The uncertainty in the range coming from an inaccurate calculation of the energy deposited in matter per unit path length (by using the WEPL approach) and the uncertainty in the positioning of the patient.

2b. Representation of uncertainties: To each voxel assign a new WEPL value by sampling from the assigned pdf's. One instance of the sampled error is used for all the voxels having a HU value below -300. Another instance to those having a HU value greater than 700 and another instance for HU values in between -300 and 700. The mean value of the pdf is set to be the nominal value give in the HU-to-WEPL calibration. The variance of the pdf will be chosen in a way that represents the *degree of belief* in the dose calculation. For the cases presented in this section and the following a rectangular (uniform) pdf will be used. The width of the rectangular pdf should be in accordance with the value of the relative uncertainties discussed above.

2c. Representation of uncertainties: The value of the shift of the patient form its ideal position (misalignment) will be sampled from the double gaussian discussed above.

3. Uncertainty propagation: Perform a forward calculation using the energies and weights calculated in step 1. Store the resulting dose distribution.

4. Dose histogram construction: Go to step 2a and repeat until a predefined number of dose distributions N_{max} has been collected. For the following cases a value of $N_{max} = 100$ was used.

The method was applied to the Head and Neck case shown in Figure 2.14. The method was used for the construction of the PTV in two different plans: a plan using two horizontal opposing beams and a plan using two oblique beams with angles of 60°

[1]Based on the experience gained by practice a physicist could use better initial guesses. This would reduce the number of iterations necessary to construct the final PTV.

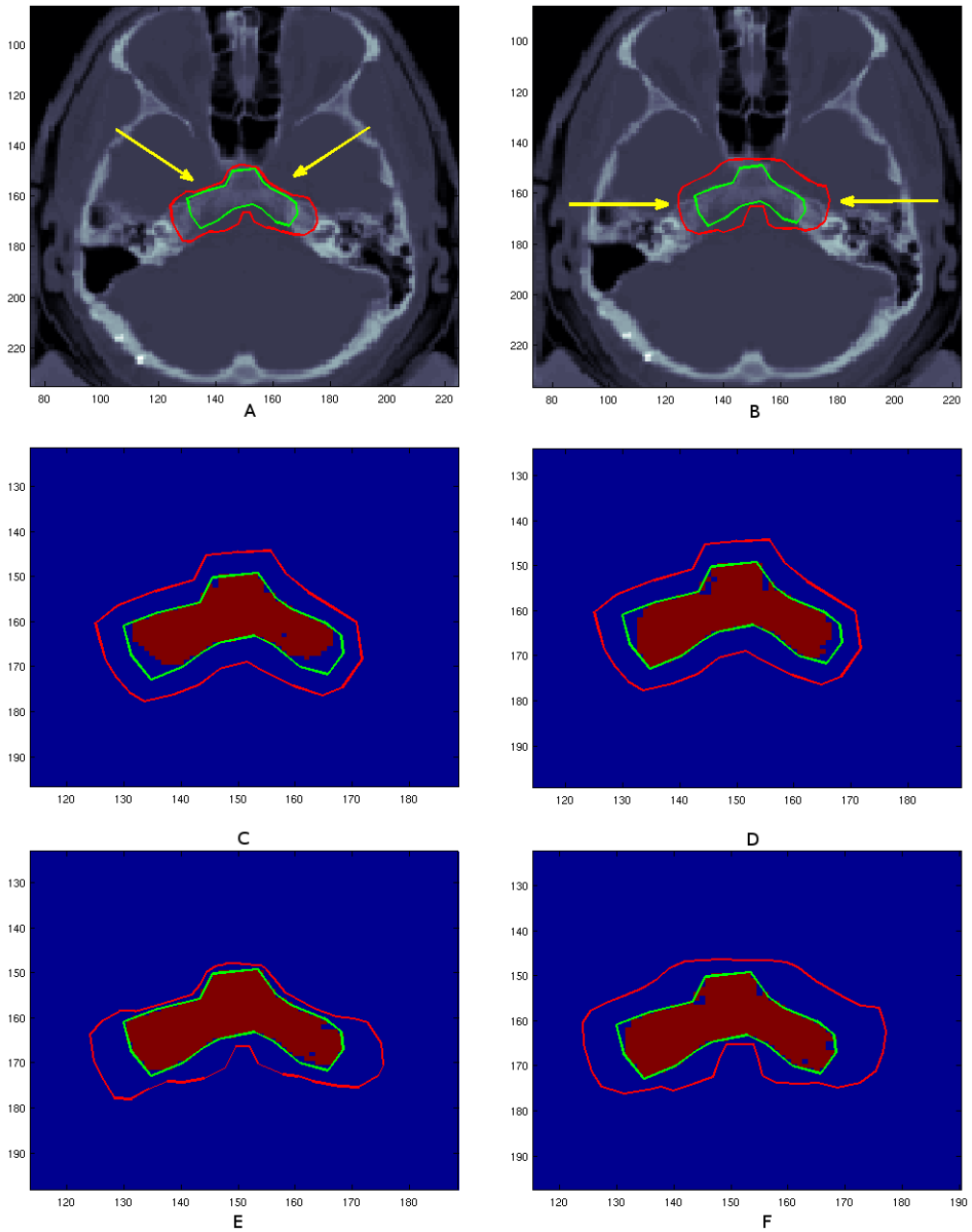

Figure 2.14: Head and Neck case - Volume expansions with the proposed approach (A)(B)(E)(F); and with a 5 mm margin (C)(D). Figures (A)(C)(E) are for an oblique irradiation and Figures (B)(D)(F) for a horizontal (two opposing beams) irradiation. Contours in red correspond to PTVs and contours in green correspond to CTVs. In Figure (C)(D)(E)(F) voxels in red are considered to be safely treated under m=5 and v=3.

and 300° . Figure 2.14 shows the obtained PTV(5,3) and the tCTVs(5,3) resulting from such PTVs. For comparison it also shows the obtained tCTVs(5,3) after planning on a 5 mm isotropic margin expanded PTV. In all the cases the results are for one iteration (one histogram generation) and to the shown tCTVs no compactification operations were applied.

Figure 2.15 shows the *mean dose distribution* and *uncertainty dose distributions* both normalized to the prescribed dose.

One can see that:

- Beam direction has an effect on the robustness of a plan. Even with an isotropic expansion the percentage of CTV voxels being safely treated changes considerably with the beam arrangement.
- The approach presented here produces planning target volumes that change dynamically in size and shape with beam orientations. This should not be a surprise since in the dose calculation engine range uncertainties are dependent on the HU values that the beam has to go trough and miss-positioning errors, seen as movements, have a larger component in some directions than other.
- The approach presented here enhances the percentage of CTV voxels safely covered as compared to the isotropic expansion.
- Under the presented method, the most robust beam arrangement will produce a smaller PTV expansion. This result is logical. The tCTV volume of non-robust beam arrangements will be smaller than the tCTV of robust beam arrangements. This means that there is a one-to-one relationship between the robustness of a plan coming from its beam arrangement and the PTV size generated with the method.

Table 2.3 shows these features:

2.3.2 A Prostate case

The method was also applied to a two dimensional prostate case. The sources of uncertainties and their modeling are the same as in the previous case. Again, two beam arrangements were used. One with two horizontal (opposing) fields and one with

Plan #	Type of expansion	Beam arrangement	PTV size (in voxels)	% of CTV safely covered
1	5 mm margin	Horizontal	1004	90
2	5 mm margin	Oblique	1004	83
3	Proposed method	Horizontal	1140	95
4	Proposed method	Oblique	909	98

Table 2.2: PTV sizes and percentage of CTV safely for the H&N case, treated from volumes in Figure 2.14.

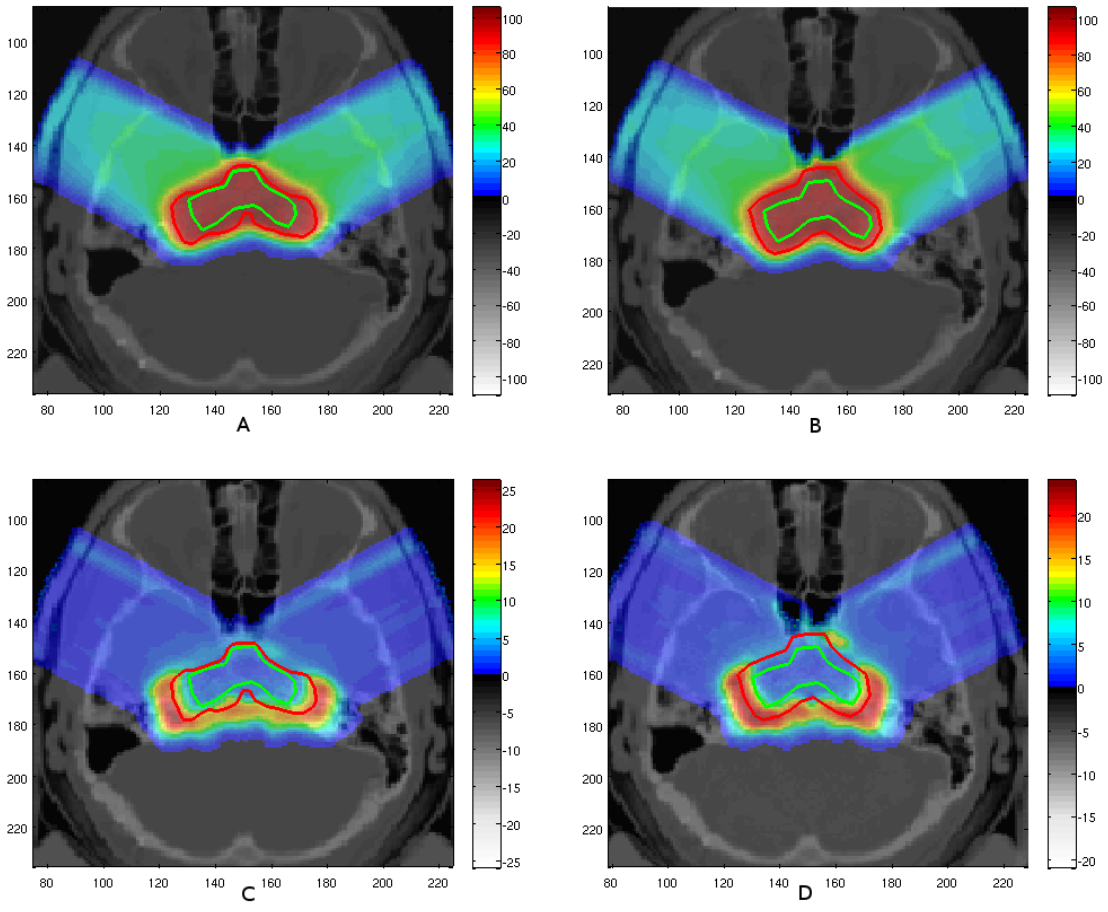

Figure 2.15: Head and Neck case - Mean dose distributions and uncertainties for Plans #2 and #4 shown in Figure 2.14

an oblique set of beams (45° and 315°). For comparisons the results are also presented for the case of a PTV obtained by applying a 6 mm constant margin to the CTV, so a total of four plans were calculated. In every plan a SFUD technique was used. Figure 2.16 shows these results. Results with the proposed approach are shown for one iteration.

As in the previous case we can see that different beam arrangements were affected to a different extent by uncertainties. The PTVs generated with the proposed method produced different beam expansion depending on the beam configuration used. For both beam configurations the number of CTV safely covered was enhanced as compared with number of voxels safely treated with the use of a constant margin. Once again, the most robust plan had also the smallest PTV (Plan # 8).

Plan #	Type of expansion	Beam arrangement	PTV size (in voxels)	% of CTV safely covered
5	6 mm margin	Horizontal	1451	84
6	6 mm margin	Oblique	1451	64
7	Proposed method	Horizontal	1352	90
8	Proposed method	Oblique	1312	99

Table 2.3: PTV sizes and percentage of CTV safely for the prostate case, treated from volumes in Figure 2.16.

Due to the fact that the volume expansion generated with the proposed method changes with some of the parameters of the plan, such beam angle arrangement and beam spots modulation[1], the target expansion proposed will be referred to as *Dynamic Target Definition (DTD)*.

2.3.3 Robust conformity indexes

Having explained the idea behind Dynamic Target Definition let's revisit for a moment the concept of the *conformity index*. The conformity index as a quantifier of conformal dose coverage to the PTV was motivated with the arrival of 3DCRT and IMRT in photon therapy. As it was discussed earlier, this modalities are less sensible to errors and uncertainties than ion beam therapy. The question is: just as the standard way of generating a PTV[2] might not be adequate in Ion Beam Therapy, is the notion of conformity as we know it also adequate? It is said that proton and ion beam therapy

[1] This will be discussed in next sections.

[2] As reported in the ICRU 50 and 62(57, 58).

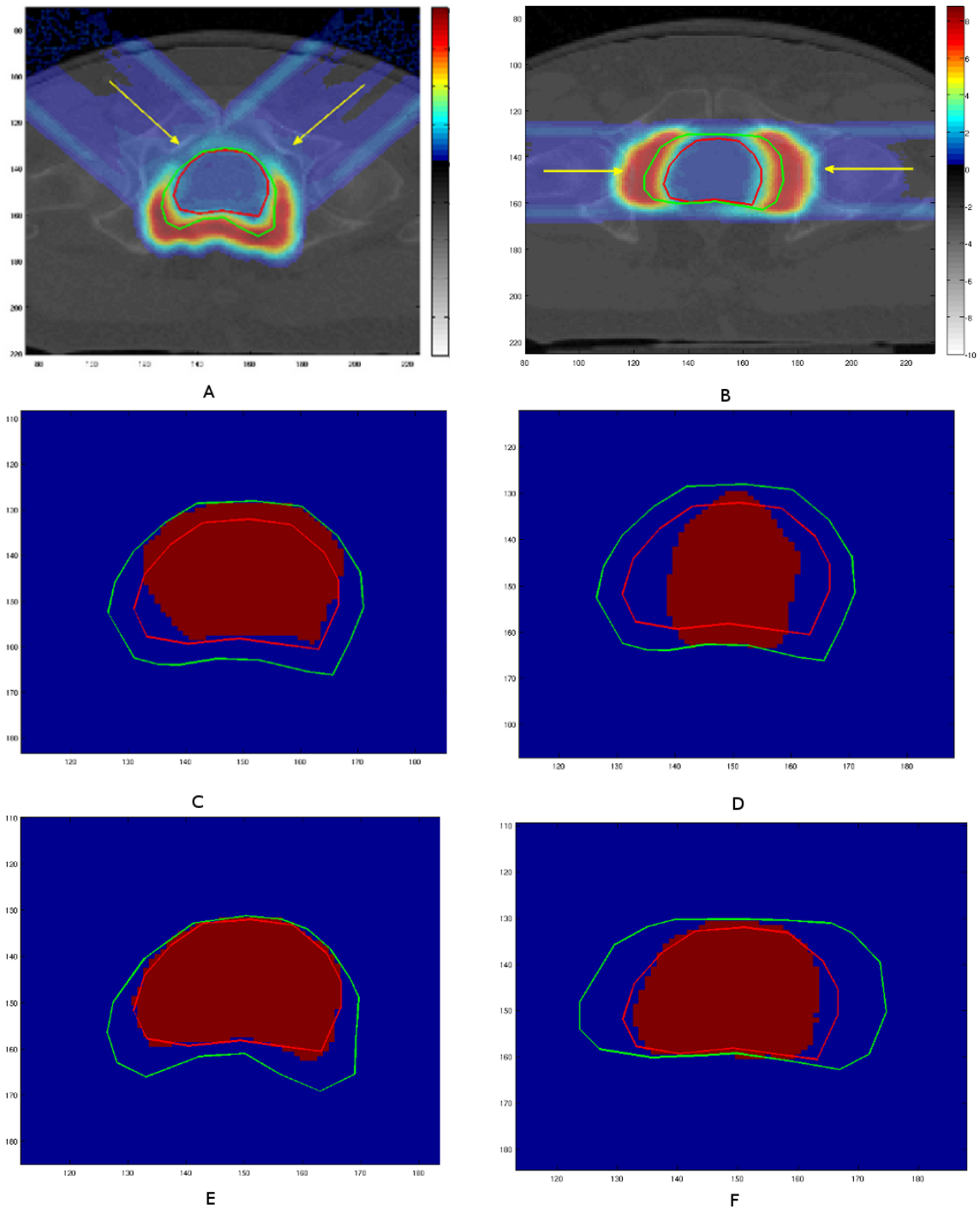

Figure 2.16: Prostate case - Volume expansions with the proposed approach (A)(B)(E)(F); and with a 6 mm margin (C)(D). Figures (A)(C)(E) are for an oblique irradiation and Figures (B)(D)(F) for a horizontal (two opposing beams) irradiation. Contours in green correspond to PTVs and contours in red correspond to CTVs. In Figures (C)(D)(E)(F) voxels in red are considered to be safely treated under m=5 and v=3. In Figures (A)(B) the dose uncertainty distribution is shown.

are highly conformal modalities. Decades ago, no other type of external radiation therapy was matching the ability to tailor a volume with high dose regions[1]. Nowadays, highly conformal therapies are achievable using photons. The question however is not just about how conformal a dose distribution appears to be in a Treatment Planning System. The question is: how much can the dose distribution estimated by the TPS be trusted? To what extent *what we see is what we get?*. How conformal is the dose distribution in the presence of uncertainties? How *robust* is the conformity?

To answer these questions in a quantitative way let's define the following: The volume M consisting in those voxels safely treated that belong to the PTV(m,v) but not to the CTV:

$$M(m,v) = PTV(m,v) \setminus CTV \tag{2.4}$$

The fraction of CTV voxels that are safely treated:

$$R = \frac{\text{Size of the tCTV(m,v)}}{\text{Size of the CTV}} \leq 1 \tag{2.5}$$

The number of voxels safely treated that belong to the PTV(m,v) but do not belong to the CTV. This number is normalized to the number of voxels of the CTV:

$$C = \frac{\text{Size of the M(m,v)}}{\text{Size of the CTV}} \geq 0 \tag{2.6}$$

Ideally one would like uncertainties to not affect significantly the dose coverage of the CTV. That means, a tCTV as close to the CTV as possible. This is the basis of the idea of robustness towards CTV coverage that motivated the concept of target expansion and it is quantified by the R value in Equation 2.5. This value ranges from 0 to 1, being 1 the optimal value.

At the same time, it is desirable that the volume of voxels safely treated does not expand beyond the CTV. Although it is always the case that the treated volume is larger than the CTV, the reason for an expansion is not to ensure robust coverage outside of the CTV. For this reason a C value close to 0 is the optimal value. Table 2.4 summarizes the values of CI, R and C for the eight cases shown above.

[1]In modern photon therapy however the level of conformity is comparable to the one obtained in ion beam therapy

Plan #	Type of expansion	CI	R Index	C Index
1	5 mm margin	1.11	0.90	0.00
2	5 mm margin	1.11	0.83	0.00
3	Proposed approach	1.09	0.95	0.00
4	Proposed approach	1.14	0.98	0.00
5	6 mm margin	1.06	0.84	0.23
6	6 mm margin	1.06	0.64	0.10
7	Proposed approach	1.10	0.90	0.00
8	Proposed approach	1.12	0.99	0.00

Table 2.4: Comparison of the CI, R and C values for the H&N and the prostate case.

One can be seen that R values obtained by isotropic expansions are the lowest. In the prostate case, the C values were non-zero meaning that not only the CTV coverage might have been compromised but that also an unnecessary large volume of healthy tissue was irradiated with a large dose.

Table 2.4 shows how the values of CI are particularly similar in all the plans studied. It also shows that the conformity index CI is not a good quantifier of the *robustness of the conformity*. The robustness of the conformity can be very well characterized by the R and S values. It is worth noticing how for Plan # 4 and Plan # 8 the value of R and C are nearly optimal. In this work this feature will be referred as ***robust conformity*** and the indexes R and C, as their quantifiers, will be referred as ***Robust Conformity Indexes***.

2.3.4 What about IMPT?

In the cases shown above the treatment modality was proton therapy with an active scanning delivery system. The technique used was SFUD. A natural question then arises: What about IMPT?

Let's apply the DTD to two different IMPT plans: oblique plan an opposing field beam plan. Figures 2.17 show the results of a modulated prostate plan with the oblique (45° and 315°) beam arrangement and Figure 2.18 shows the results for the horizontal beam plan. The sources of uncertainties used and their values remained the same as in previous section. Figure 2.18 shows a nice and compact tCTV volume generated. The existence of such volume is the *heart* of the DTD method and the rationale of the PTV

concept. However Figures 2.19 and 2.20 show a very different type of result. Under this specific IMPT plan protons are stopping near the center of the CTV. This leads to high uncertainty regions inside the CTV as opposed to having them in the distal edge. As a consequence, the standard deviation of the histogram will be large and a significant volume of CTV voxels will not be safely treated. That however is not the worse part. The real problem is that under the specific beam modulation the tCTV will no longer be a large, compact subvolume!. The case shown in Figure 2.20 did not generate a compact subvolume for values of $v < 9\%$ and even for this value, the tCTV is quite small, meaning that a very large expansion would be necessary. If we agree that a lower value of v should be used then inevitably we find ourselves in an uncomfortable position. Did the method fail? Not really. What really failed is *the concept* of target expansion as a method to ensure robust dose coverage in the CTV: the PTV concept.

This problem was recently reported by Albertini et al (68). Some of the concepts developed for conventional photon therapy are being pushed beyond their limits in ion beam therapy, being this concrete case a good example. As far as the PTV concept goes, it can be a useful tool to deal with uncertainties in Ion Beam Therapy. However a more reliable and complete solution to the robustness problem will more likely involve additional steps in the planning procedure and inverse planning. A good example is the work of (69, 70, 71, 72), who use robust optimization methods to obtain the beam spot modulation. These approaches manage to minimize the variance of the dose in the CTV voxels. A combination of such features with the DTD could hopefully prevent us from delivering expansions that do not assure their purpose. This is however a topic for future work and it will be reported elsewhere.

2.3.5 A framework for robust treatment planning in Ion Beam Therapy

In the previous sections it was shown how beam spot modulation, beam arrangement, treatment plan robustness and PTV definition have intrinsic connections.

The ideas presented above provide not only a tool for creating a margin expansion but also introduce a conceptual layout to deal with the dependencies in treatment quality and robustness. It is clear that under this framework, the PTV is not a static volume define prior to inverse planning and beam arrangement definition but instead

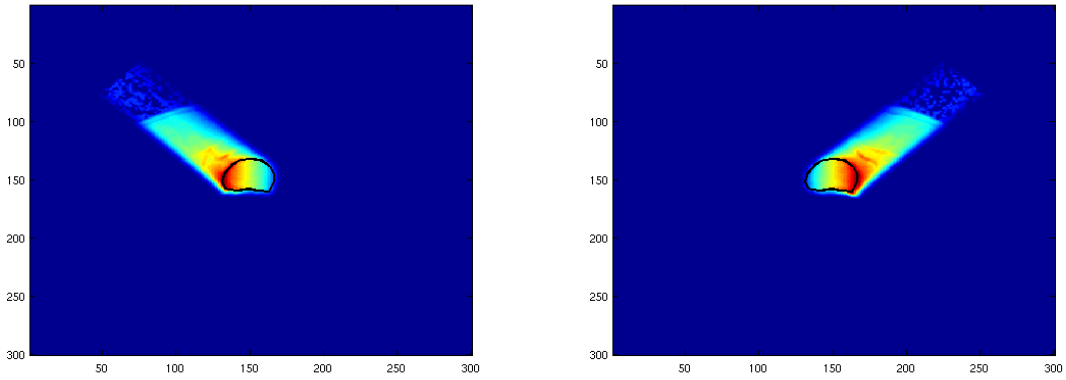

(a) Beam #1 **(b)** Beam #2

Figure 2.17: IMPT oblique plan for the prostate case.

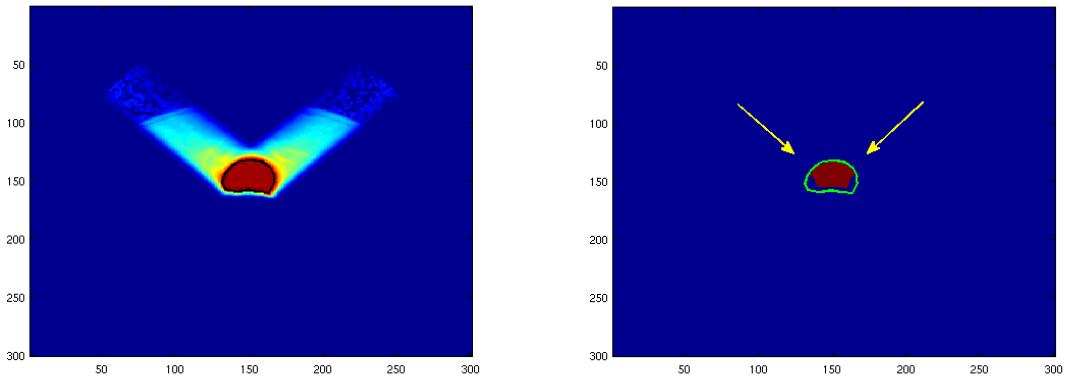

(a) Total dose distribution **(b)** tCTV(m=5%,v=3%)

Figure 2.18: Total dose and tCTV for the IMPT plan of the prostate case.

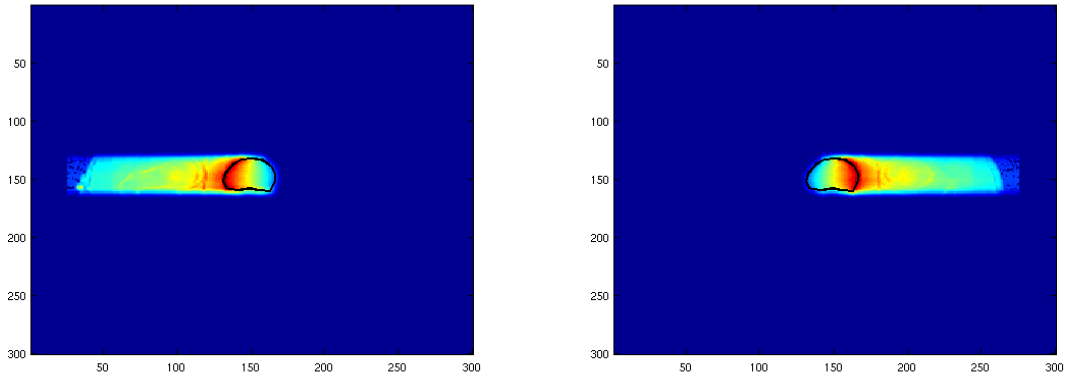

(a) Beam #1 **(b)** Beam #2

Figure 2.19: IMPT horizontal plan for the prostate case.

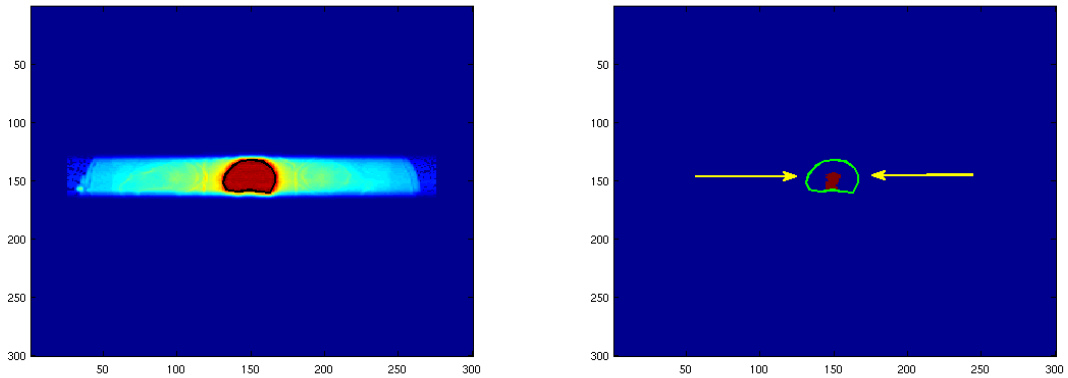

(a) Total dose distribution **(b)** tCTV(m=5%,**v=9%**)

Figure 2.20: Total dose and tCTV for the IMPT plan of the prostate case.

it it shows its dependencies in a convoluted way. Having this in mind it is fair to ask: How should the work flow of treatment planning should look like under the DTD?

Figure 2.21 shows a proposal for robust treatment planning in Ion Therapy. It consist of four phases:

Data acquisition: In this phase the relevant data and information is acquired. Some of these data are: Patient images from different modalities, contoured CTVs and OARs, constraints for the OARs, types of uncertainties to be taken into account along with their probability density function and robustness constraints in the form of the parameters m and v used in the previous sections. Also, the beam arrangements are selected here. This could be done manually or by using a beam angle selection algorithm[1]. Beam spot modulation is also defined here. This should be done, ideally, with the assistance of a probabilistic tool for inverse planning.

Uncertainty propagation: In this phase the histogram of dose calculations is generated and stored.

Impact on Coverage and Target Expansion: In this phase the impact on CTV coverage is assessed by the calculation of the tCTV(m,v). Having that, the PTV(m,v) is also generated iteratively until $tCTV(m, v) = CTV$.

Clinical assessment and approval: In this phase several aspects are checked for approval: constrains to the OARs, PTV size and general plan feasibility. If the requirements are met the plan is approved. If not, the process resets some of the relevant plan parameters (like beam arrangement) and starts over.

Figure 2.21 shows a differentiation in the type of steps that conform the flowchart. Boxes in green are meant to be done by a radiation oncologist or therapist. Boxes in yellow by experienced treatment planner and physicist and boxes in gray are done automatically under the hood by the treatment planning system.

[1]This matter will be addressed in Chapter 3.

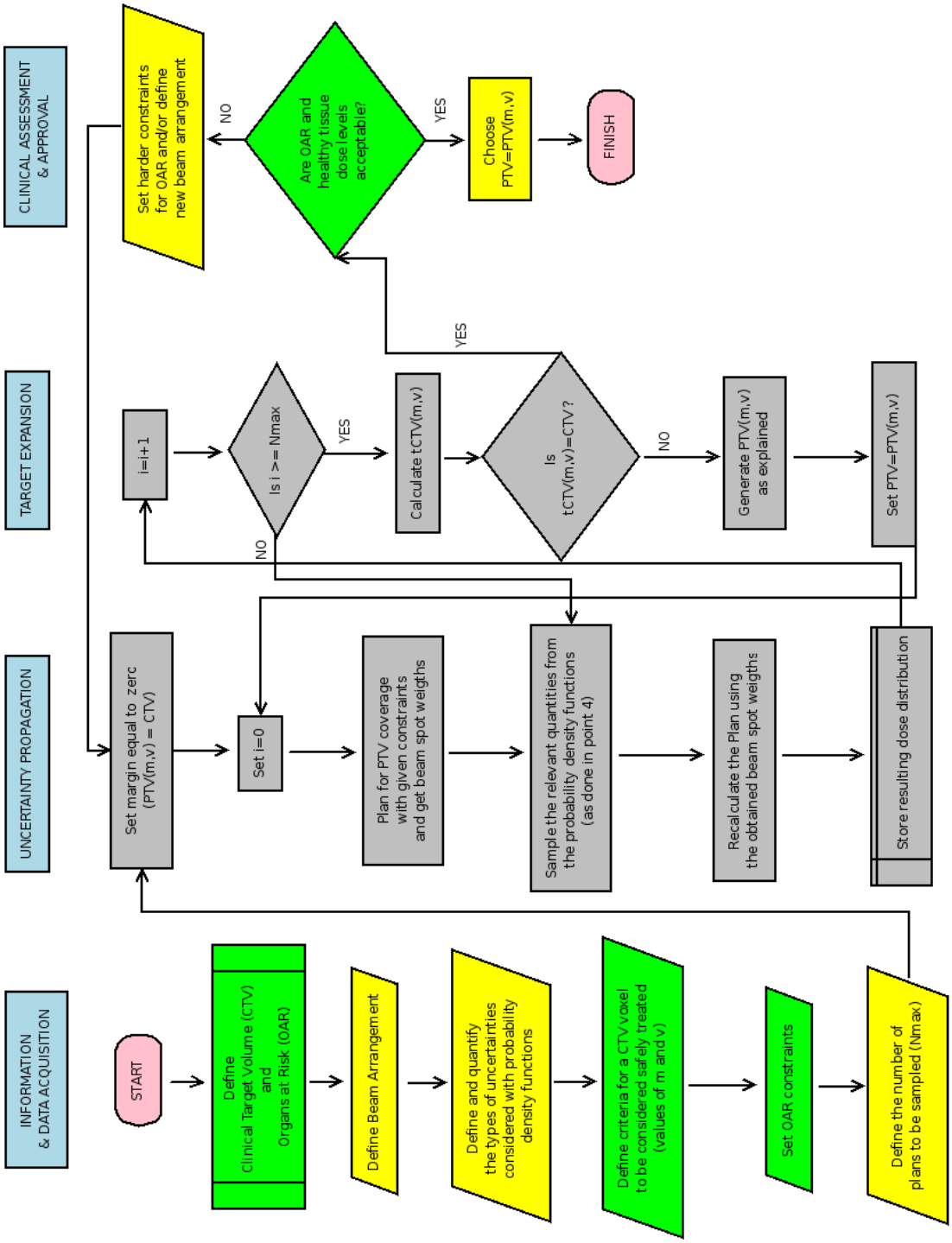

Figure 2.21: Flowchart of the proposed planning procedure - Boxes in green are meant to be done by a radiation oncologist or therapist. Boxes in yellow by experienced treatment planner and physicist and boxes in gray are done automatically under the hood by the treatment planning system.

2.4 Discussion

The need for PTV has been identified and investigated for a long time (57, 58, 60, 61, 62). From its beginning the concept was developed to assure robustness towards CTV coverage. It is a concept initially developed to mitigate the impact of uncertainties in conventional photon therapy.

The convenience of the method for 3DCRT and IMRT is probably still an open question.

Particularly for ion beam therapy with an active delivery system, the standard expansion rule fails to address the problem of uncertainties. This problem has been identified and countermeasures are being proposed to reduce the sensitivity of plans to these errors. Of particular interest is the use of robust inverse planning as done in (69, 70, 71, 72, 73).

In this chapter a method was proposed to assess if the PTV concept addresses the issue of robustness and, if so, to reduce the impact of uncertainties on the CTV dose coverage, under the specific parameters of the plan such like beam spot modulation and beam angle arrangement.

Having this in mind CTV-to-PTV expansion in ion beam therapy should be a dynamic process within treatment planning and a result of a successful planning procedure, rather than its starting point. Dynamic Target Definition provides a framework in which the planner dynamically experiences how PTV size, plan robustness, beam spot modulation and beam arrangements are convoluted concepts that are depend on each other. The approach presented here makes it easy to understand the limitations and the advantages of a treatment modality and of the PTV concept itself.

Several authors have studied the impact of uncertainties on the dose. Unkelbach and Oelfke (74) used Bayesian inference to assess the impact of organ motion in dose uncertainties. Maleike et al (75) simulated and visualized dose uncertainties for interfractional motions. Lomax (50) used histograms of dose distributions and assessed their sensitivity to interfractional errors by analyzing the worst dose scenario obtained at each voxel.

In this chapter we have used dose histograms for the quantification of the sensitivity of plan to errors and uncertainties. Once a histogram was generated the values for the

standard deviation v and the mean deviation m were used. It is worth mentioning that these values play a crucial role. The use of m=5% and v=3% is due to the fact that they approximate well the 95%-107% limits for PTV irradiation recommended by ICRU 50(57). In principle any other choice can be used, if justified. The fact that these parameters are directly connected to the dose distribution and its uncertainties makes the overall approach very transparent. The values used for the WEPL uncertainties presented here are not meant to be used in clinical practice but rather an explanatory guide on how to apply them once they are known. The basic guideline we used for deriving such values are based on (16).

It has been discussed in the literature (24, 45, 67) that the technique used for irradiation with an active delivery system, whether is SFUD, IMPT or DET has an impact on plan robustness. Within the DTD approach this means that the generated PTV will be specific of the technique used. Recently it has been reported (68) that in IMPT plans requiring high levels of beam spot modulation (like it might be the case if very hard OAR constraints are applied) the standard concept of CTV-to-PTV margin might not be enough in order to assure CTV coverage. This is in agreement with the proposed approach since high levels of modulation without taking into account robustness might lead to tCTV(m,v) volumes that are too small.

An important question is of course, how an appropriate sparing of healthy tissue can still be achieved when using this method. In ion beam therapy is usually easier to spare healthy tissue from medium and low doses as compared to photon treatments. Having said so, the DTD approach can be connected to an IMPT optimization and/or to a Beam Angle Optimization algorithm[1]. Ideally, further consideration on plan robustness could be added in the beam spot weight optimization process itself as done in (69, 70, 71, 72). By doing so the PTV(m,v) volume generated is expected to be even smaller while achieving the same level of dose CTV coverage.

It is worth mentioning that since there is a direct connection between the volume of the PTV(m,v) generated and the robustness of the treatment plan, the size of this volume becomes a very attractive objective the function for robust optimization. This

[1]This will be discussed further in Chapter 3

feature should not be overlooked. One of the main challenges in developing an algorithm for robust optimization is to find an objective function that directly or indirectly relates to the uncertainties taking into consideration. By using the PTV(m,v) size as such function we guarantee that any source of uncertainty can be easily taken into account once it has been characterize with a probability density function. This feature will be studied further in Chapter 3.

A full Monte Carlo based uncertainty assessment as was done here might not be always efficient in terms of computing time. In order to realize a histogram of dose values for each voxel, several forward dose calculations have to be performed which means that the required calculation time is proportional to the time it takes for a forward dose calculation. Modern algorithms can perform a forward calculations in seconds which means that PTV generation can be done within few minutes. Of special interest is the use of a bootstrap resampling strategy to create the dose histograms. Another way to attack the problem is to try to calculate directly the uncertainty maps. In some cases these calculations might be fairly well approximated by analytical expressions. Despite the fact that each histogram generation involves several dose calculations, the method converges very fast. The results presented were achieved within two iterations (two sets of N_{max} dose distributions).

The method can be also applied to take into account internal organ motion. The case is particularly simple for organs in which the motion is periodic and well characterized by the use of 4D CT.

A constant RBE along the Bragg Peak was used in this chapter. In the last years authors have discussed how the increasing RBE of protons in their distal end might cause an "effective biological range" larger than expected (76, 77, 78). This scenario was not treated in this analysis and is left for future investigations.

In DTD range errors which are mainly systematic are treated as random errors. By randomizing these systematic errors one takes a Bayesian approach in which uncertainty is attached to the degree of belief about a given quantity rather than to random fluctuations of it. This allows to combine systematic and random errors within an unified framework. By doing so, one obtains uncertainty maps that allow us to visualize the degree of belief we can have on dose calculated in each voxel. This is a feature that

has an immense value and has been pointed out by several authors (74, 75). We believe it will play an important role in treatment planning in the 21^{th} century.

3

Robust beam angle selection in Ion Beam Therapy

"If there is a problem you cant solve, then there is an easier problem you can solve: find it."

George Polya

This chapter builds on some of the concepts introduced in Chapter 2 to attack a problem that has gained considerable attention over the last few years: the problem of beam angle selection. Rather than giving a generic solution for all types of external radiation therapy, this chapter will treat this problem for the specific case of ion beam therapy.

3.1 Beam angle selection in radiation therapy

The possibility to rotate the treatment table and the gantry independently opened up the option to choose beam angles from almost any arbitrary direction. During many years of conventional radiation therapy, class solutions based on the experience of the clinicians were used for each specific site of irradiation. From the arrival of IMRT and the tools for inverse planning, many researches have tried to solve the beam angle selection problem as an inverse problem. In the literature the term *Beam Angle Optimization (BAO)* often refers to it. In the last years the word *optimization* has probably been one of the most overused term in treatment planning. The natural enthusiasm from the successful story of inverse planning in IMRT has led many to

believe that the BAO problem can be solved by using similar methods. But so far the problem has proven to be very challenging. The reason is the following: There are two generic ways to handle the inverse BAO problem:

1. The first way would be to provide an analogous formulation to the inverse IMRT problem. That is for every beam configuration and every intensity modulation use the function:

$$D_i = F(\vec{\phi}_1, \vec{w}_1, ..., \vec{\phi}_N, \vec{w}_N) \tag{3.1}$$

   where $\vec{\phi}_k$ defines the beam direction of the k^{th} beam, $\vec{w}_k$ is the intensity modulation for that field and D_i refers to the dose in an arbitrary voxel.

   Using such function F one could, in principle, minimize the deviation of the dose D_i from a desired dose D_{des} just like in the familiar problem of intensity modulation. The main problem is however that the search space for such problem is enormous. Not only the combinations of beam configurations would have to be taken into account but also the intensity modulation of every field is dependent on the beam arrangement itself. From the mathematical point of view this is a very complex problem.

2. The second strategy involves the use of heuristics approaches to find solutions without having to navigate in the immense search space of the previous problem. In this case the merit of a beam angle configuration is often evaluating based on anatomical or geometrical considerations, avoiding the need of having to perform a dose calculation for every possible scenario. This way the complexity of the problem is reduced however the validity of the whole approach depends on the heuristics used. The choice of an appropriate quantifier of beam angle merit is a sub-problem that needs to be addressed.

Is easy to understand the complexity of both approaches when looking at what has been published. Already in the 90's research on this area was published (79). Often, researches have put their attention on vigorous methods borrowed from the field of Machine Learning like stochastic algorithms (80, 81, 82, 83, 84, 85, 86), artificial neural networks (87) and other modern techniques (88, 89, 90, 91). Recently, Bangert and

Oelfke (92) proposed a heuristic approach in which they identify clusters of optimal solutions on the sphere via spherical K-means algorithm.

To make things even more challenging, it has been recognized (45, 50, 70) that (particularly in ion beam therapy) the issue of *plan robustness* needs to be taken into account. Several authors have proposed methods for robust treatment planning. Unkelbach et al (69, 70) proposed a probabilistic approach for inverse planning in proton therapy while dealing with the uncertainties in proton range in a generic way. Pflugfelder et al (71) proposed a worst case optimization to account for range errors and set up uncertainties, similarly Fredriksson et al (72) used a minimax approach to reduced the impact of uncertainties over large set of possible scenarios and recently Chen et al (73) used multi criteria optimization (MCO) to find a compromise between dose sparing and plan robustness[1]. These works all share that they have not taken beam angle configuration as input parameter to be optimized.

3.2 A proposal for a robust beam angle selection in Ion Beam Therapy

Given the nature of the dose deposition of ion beams, beam angle selection plays a crucial role in the quality and robustness of a treatment. While in IMRT the increased number of fields and the intensity modulation are used to guarantee steep dose gradients, they also guarantee a high volume of medium and low dose. The situation is different in particle therapy where very few beams can achieve a conformal dose coverage. At the same time if an OAR is irradiated it is because either one of the beams went through it or it is located in the close vicinity of the target. Geometrical considerations could prevent at least, the first of these two scenarios.

Geometrical considerations can also enhance plan robustness. For instance some materials might have a greater uncertainty in their stopping power (or WEPL) than others. Avoiding going through them would increase the overall robustness of the plan. As was it shown in the Introduction, the impact of set up errors and movements on plan robustness is also dependent on the type of interfaces that the beam goes through

[1]The validity of this approach will be discussed below.

(44, 45, 50). Avoiding such directions decreases the uncertainty in the position of the beam spots.

From this perspective it is clear that the strategy of angle selection *as way to enhance robustness* is worth investigating. In this section a method for robust beam angle selection is presented. It can be used for treatment planning using either a passive or an active delivery system. Here the application of the method on an active delivery system is limited to the SFUD technique. A discussion on the perspective of the use of the method for IMPT will be given at the end of the chapter. The method is based on three postulates that will be followed through the development and implementation of the algorithm. The three postulates are:

Robustness is a priority : The robustness of a plan is not just a desirable attribute, it is a mandatory prerequisite. It reduces the space of possible beam and intensity configurations to a subset upon further optimization can be carried out. If possible, it should be a hard constraint rather than a soft constraint. To talk about finding "a compromise between robustness and treatment plan quality (meaning conformity and healthy tissue sparing in nominal plans)" is in itself a contradiction. The robustness of a plan is a measure of how much can the plan shown on the screen be trusted. Having a beautiful nominal plan with a compromised degree of robustness is like being proud of a point estimate while ignoring overwhelming error bars. In this sense one should be very careful with strategies that address this problem as multi criteria. One can ask a clinician if he prefers a slight overdose in the bladder over an overdose in the rectum. That is a compromise. But uncertainty and degree of belief can not be compromised, *never*. It is not a clinical decision, it is a profound epistemological question.

The size of the tCTV is a measure of robustness :[1] In Chapter 2 it was pointed out that the size of the PTV(m,v) was a measure of robustness of the beam arrangement[2]. The size of the PTV(m,v) is inversely proportional to size of the tCTV(m,v). Is given by the number of voxels in the CTV that are not sensible to errors in terms of dose coverage. It is not a heuristic quantity neither a surrogate

[1]The tCTV concept is explained in Chapter 2. Here we will refer to the tCTV as the compact set of voxels safely treated when planning *on the CTV*. This allow us to find a beam arrangement before making a PTV expansion. The values of m and v used will be 7%.

[2]Under a SFUD technique.

of plan robustness. It defines it. By using the tCTV as measure of robustness we avoid the need to establish a quantifier of robustness for each of the sources of uncertainties that are taken into account. The fundamental step is to be able to give a bayesian characterization of the uncertainties as discussed in Chapter 2.

Beam angle selection and PTV definition should be connected : From a conceptual point of view, if two strategies are used to deal with robustness (beam angle selection and PTV definition), these strategies should work synchronized. The PTV concept was born as an early attempt to deal with uncertainties. As shown in Chapter 2, for two different plans having different levels of robustness, different PTVs are needed. If a beam selection reduces the impact of uncertainties, an appropriate PTV should be used. Having a generic PTV might in some situations compromise the dose in structures that are close to the CTV and in some cases it might not even be an efficient way to mitigate the consequences of errors.

3.2.1 Objective function for one-beam robust selection

In this paragraph we propose a method to derive the most robust beam configuration. Let's call $\vec{\phi}$ an arbitrary beam angle direction in a three dimensional geometry. The vector $\vec{\phi}$ has two components: one defining the azimuthal angle and another one defining the polar angle. The objective function quantifying the value of a given direction in terms of robustness will be:

$$R_{tCTV}(\vec{\phi}) = \mu(CTV) - \mu(tCTV(m, v, \vec{\phi})) \tag{3.2}$$

where $\mu(.)$ is a function returning the volume of the structure in units of voxels. The function R_{tCTV} will have values ranging from zero to the number of voxels found in the CTV. The task is to find such $\vec{\phi}^*$ that:

$$\vec{\phi}^*_{tCTV} = \underset{\vec{\phi} \in S^2}{\arg\min} R_{tCTV}(\vec{\phi}) \tag{3.3}$$

Minimizing function R_{tCTV} brings a computational challenge. For every beam direction one would have to generate a histogram of dose calculations as the ones done in Chapter 2. For that reason it is useful to find a second function R_s that behaves like

R_{tCTV} does, that is, that increases as R_{tCTV}, decreases as R_{tCTV} decreases and have the local and global extremes in the same points in search space.

Let's assume that a given beam uses M beam spots. The position of the j^{th} beam spot in a nominal plan will be given by the vector $\vec{s}_j^0$. Let's describe the errors and uncertainties by using probability density functions. If we sample one instance of these errors (such as set up or range errors) and calculate the location of the j^{th} beam spot under that realization of that error then we will obtain a new vector for the location $\vec{s}_j^k$, where k stands for the k^{th} random realization of the errors.

The quantity

$$\sigma_k^2 = \frac{\sum_j^M \left|\left|\vec{s}_j^0 - \vec{s}_{jk}\right|\right|^2}{M} \tag{3.4}$$

will give us a measure of the displacement all the beam spots under that given random realization of the error. Here M is the number of beam spots used. The average value the quantity σ_k^2 over N_{max} random realizations will define the function R_s:

$$R_s(\vec{\phi}) = \sqrt{\frac{\sum_k^{N_{max}} \sigma_k^2}{N_{max}}} \tag{3.5}$$

It is not hard to see why the function $R_s(.)$ is used as a generic surrogate of the function $R_{tCTV}(.)$. Any instance of a random realization of an error (whether it is a range error or a set up error or a motion of the organ or any other) leads to a shift in the location of the Bragg peaks within an internal frame of reference. In order to estimate the shift, the vector $\vec{s}_{jk}$ is calculated using a simple ray-tracing algorithm. The computational advantages lays in the fact that doing ray-tracing calculation for one point is much faster than performing a dose calculation for hundreds of voxels. The impact of the uncertainty on the final deviation of the dose from the one expected will generally speaking increase or decrease with the magnitude of the shift of the beam spots. This strategy allows us to use the same method for a wide range of errors and uncertainties.

Ignoring any other criteria, like healthy tissue sparing, the most robust beam angle selection for one beam would then be:

$$\vec{\phi}_s^* = \underset{\vec{\phi} \in S^2}{\arg\min} R_s(\vec{\phi}) \tag{3.6}$$

3.2.2 Objective function for multiple beams robust selection

To generalize the method to a arrangement of n beams, lets assume that the function 3.4 is evaluated for n beam angles. Let σ_{kl}^2 be the value of such function for the l^{th} beam.

Each instance of an error will affect different beams in a different way. For a given beam arrangement and a given realization of an uncertainty the most affected beam will be the one having the highest σ_k^2. This value will be referred as:

$$\sigma_k^{max} = \max\{\sigma_{k1}^2, \sigma_{k2}^2, ..., \sigma_{kn}^2\} \tag{3.7}$$

Similar to the one-beam case, the objective function proposed is:

$$R_s^{Max}(\vec{\phi}_1, \vec{\phi}_2, ..., \vec{\phi}_n) = \sqrt{\frac{\sum_k^{N_{max}} \sigma_k^{max}}{N_{max}}} \tag{3.8}$$

By minimizing this function we are practically following a minimax optimization.

3.2.3 Accounting for Organs at Risk

As opposed to photon therapy where a large volume receives medium and low doses, the tissue irradiated in ion beam therapy is located either in the entrance region of the beam or near the target volume. To minimize the irradiation of a healthy structure it is enough to avoid irradiating through it and avoid having beam spots stopping in front of it. If the only constraint to the OAR is a maximal dose constraint and the structure is located far from the target then in principle one could allow a beam to go through it as long as the dose remains below the limit. This situation is however uncommon in ion beam therapy.

The strategy for OAR sparing used here is the following:

Avoid going through organs at risk : This will avoid large volumes of medium and low dose in the healthy structure. This procedure can be automatized fairly

easy. To achieve this Jäkel and Debus (93) used a cylindrical projection of the healthy structures on the sphere of beam angle directions. Similarly Cabal et al (7) counted the number of OAR voxels through which a given beam goes. By doing so one takes advantage of the specific pattern of dose deposition by ion beams which allows to choose angles without having to perform a dose calculation.

Penalize harder beam spots shifts near the OAR : In some difficult cases the OAR is next to the target. Set up errors or errors in the estimation of the range of the particle might not only affect the dose coverage but also compromise the sparing of the OAR. Having this in mind equation 3.4 becomes:

$$\sigma_k^2 = \frac{\sum_j^M \beta_j \left|\left|\vec{s}_j^0 - \vec{s}_{jk}\right|\right|^2}{M} \tag{3.9}$$

where $\beta_j = 1$ if the j^{th} beam spot is not in the close vicinity of the OAR and $\beta_j = \beta > 1$ if it does. By doing so we are avoiding high uncertainty regions near the OAR. This is an important feature when using the DTD approach for PTV definition: avoiding high uncertainty regions near the OARs reduces the chances of having PTVs that expand onto it. This process is a generalization of the common practice of avoiding beam that stop right in front of an OAR.

3.2.4 The optimization algorithm

The function R_s is generally speaking a non-convex function with multiple local minima. Figure 3.2 shows this feature for a two dimensional Head and Neck. The search for global minima is then a difficult task. However if we focus our attention only in those regions of the search space that are clinically feasible and do not go through organs at risk the size of it reduces considerably. Jäkel and Debus (93) have shown that for a Head and Neck case the subspace of usable beam directions are just a fraction of the whole sphere. Moreover, they showed that from a clinical point of view the best beam configurations are clustered in compact regions of this subspace. For this reason we used a Newton algorithm to minimize function R_s^{Max}. The optimization was run locally in several subregions of the sphere.

3.3 A Head and Neck case

In order to exemplify the ideas discussed in the previous section they will be applied to the Head an Neck case shown in Figure 3.1.

The calculations will be done only in one CT slice so they can be regarded as two dimensional case. There are five critical structures identified: the eyes, the optic nerves and the brain stem. The target volume delineated in green is the CTV. The task is to find a robust beam arrangement of two beams while minimizing the dose in the OARs using a SFUD technique. Then to propose a PTV expansion for such beam arrangement. Notice that the distance between the CTV and the brain stem is only 1 mm.

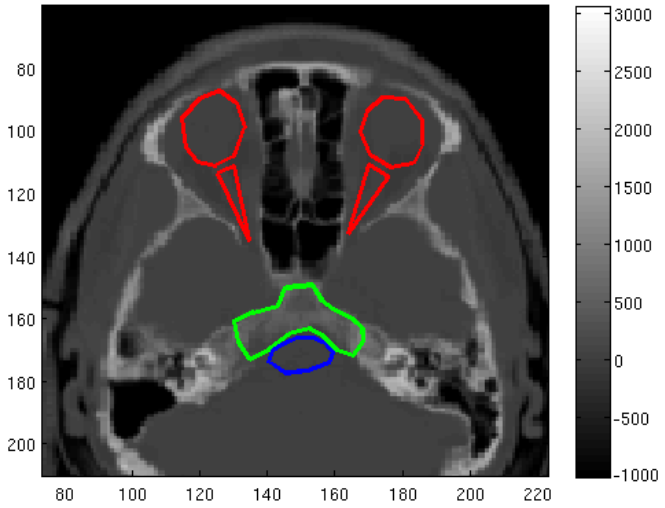

Figure 3.1: Head and Neck case - CTV is delineated in green, brain stem in blue and eyes and optic nerves in red.

In order to see the relationship between the function R_{tCTV} and its surrogate R_s their values are plot for 24 equidistant locations. In the evaluation of the function for Figure 3.2 organs at risk were not taken into account. Although we do not make use of the function R_{tCTV} the correlation between R_s and R_{tCTV} is shown in Figures 3.2 and 3.3.

Figure 3.2 shows how both functions depend on the beam angle in a similar way. Their local and global extremes are located in the same points. Figure 3.3 shows that,

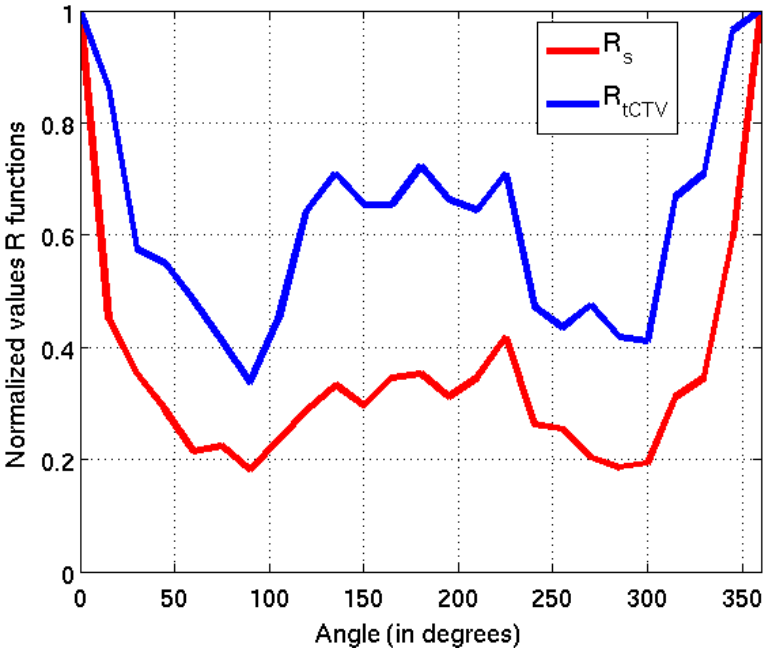

Figure 3.2: R_{tCTV} **and** R_s **for the Head and Neck case** - The functions are evaluated in 24 equidistant points

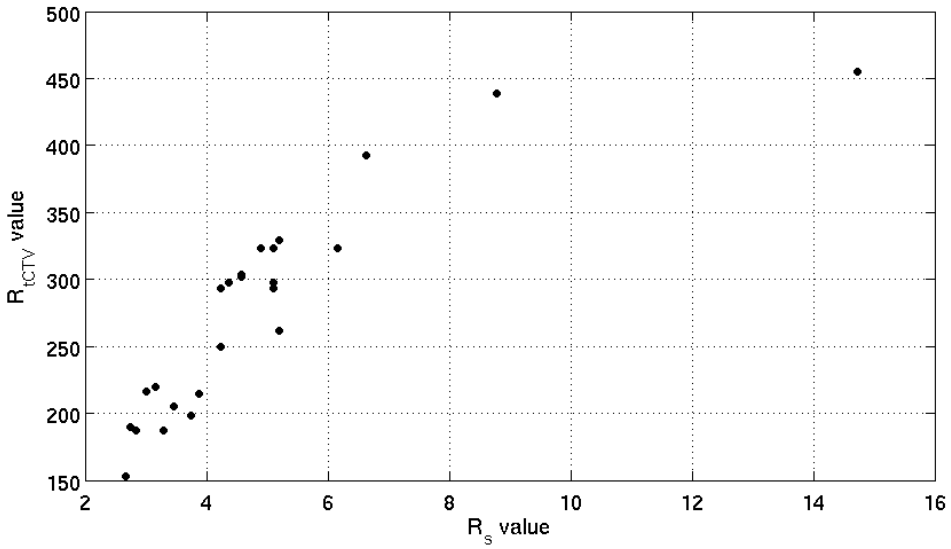

Figure 3.3: R_{tCTV} **vs.** R_s - Each point corresponds to a one-beam configuration for the 24 angles shown in the previous figure.

although there is not a one-to-one relationship between both functions their correlation is strong.

In order to look for a robust two beam configuration the function R_s^{Max} needs to be used. Again a comparison between this function and the function R_{tCTV} (now for two beam arrangements) is shown in Figure 3.4.

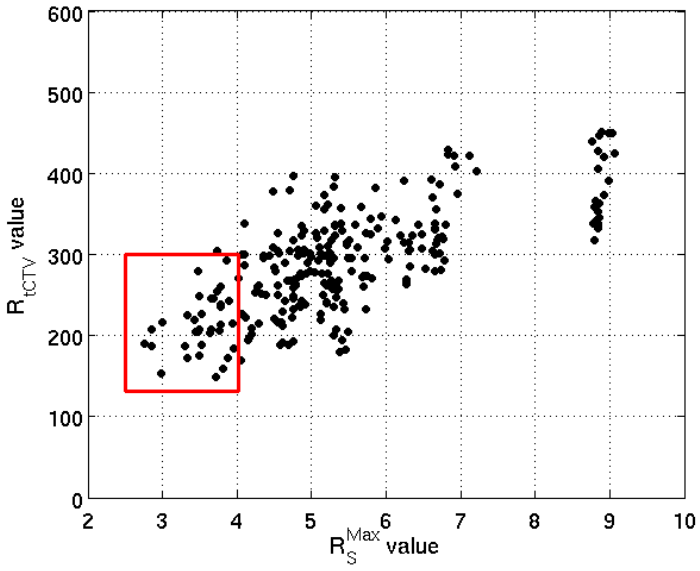

Figure 3.4: R_{tCTV} **vs.** R_s^{Max} - Each point corresponds to a two-beam configuration. The red square shows the most robust configurations.

The algorithm was run three times with three different settings:

1. In the first setting OAR were disregarded and the task was to find the most robust beam configuration towards CTV dose coverage. In this case the beam angles were discretized with a separation of 15 degrees. 276 configurations were evaluated and a local search in each of these configurations was made. The best beam arrangement obtained was $\phi_1 = 88$ degrees and $\phi_2 = 74$ degrees.

2. In the second task directions going through an OAR were avoided but no extra penalization was given to beam spot shifts near the OAR. Only fifteen initial beam configurations were allowed. A local search was performed in each of the feasible scenarios. The size of the search space was now around 20% of its original

size. The best beam arrangement obtained was $\phi_1 = 286$ degrees and $\phi_2 = 304$ degrees.

3. Finally the algorithm was run with the same search space as in the second task but using a penalization factor of $\beta = 10$ as in equation 3.9, for those beam spots that are within 5 mm of the OAR. The best beam arrangement obtained was $\phi_1 = 285$ degrees and $\phi_2 = 75$ degrees.

Figure 3.5 shows the tCTV for the first solution ($\phi_1 = 88$ degrees and $\phi_2 = 74$ degrees). Since OARs were disregarded in this run it uses a beam ($\phi_1 = 88$ degrees) that goes through an organ at risk. This can be observed on the dose volume histogram in Figure 3.9. Although the impact of uncertainties was not very high, the fact that the beam went through the OAR produced large volumes of medium-to-high dose in it.

The tCTV for the second solution ($\phi_1 = 286$ degrees and $\phi_2 = 304$ degrees) is shown in Figure 3.6. This beam configuration obviously avoids going through OARs (since this regions were excluded from search space) but places a high uncertainty region in front of the brain stem as can be seen from the figure. This can also be appreciated in the DVH shown in Figure 3.10. The fact that in the nominal plan a large number of particle are stopping in front of the OAR makes its dose assessment very uncertain, as reflected by the high fluctuations of the DVHs.

Finally Figure 3.7 shows the third solution obtained ($\phi_1 = 285$ degrees and $\phi_2 = 75$ degrees). One can see that having a penalty factor for the CTV voxels close tho the OAR reduced the uncertainty in them. This reflected not only in lowering the volumes of medium-to-high dose in the OAR (which was achieved thanks to the fact that some beam angles were avoided) but also it shows a *robust assessment* of the dose in the OAR as can be seen in Figure 3.11. It is interesting that the third solution was slightly more robust for CTV coverage than the second solution. The reason for this is that in the second solution most of the beam spots that carry the largest uncertainty are also stopping in front of the OAR. For this reason penalizing them has a two fold effect. The third solution exemplifies the algorithm proposed here and in that sense it is the solution it produces for this case. These results are summarized in Tables 3.1 and 3.2 and

The PTV defined for the optimal beam arrangement is shown in Figure 3.8.

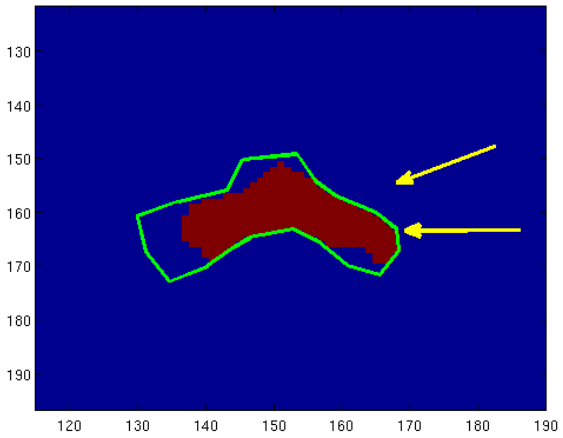

Figure 3.5: Robustness analysis for Solution 1 - The beam angles used were 88 degrees and 74 degrees. Red voxels define the tCTV.

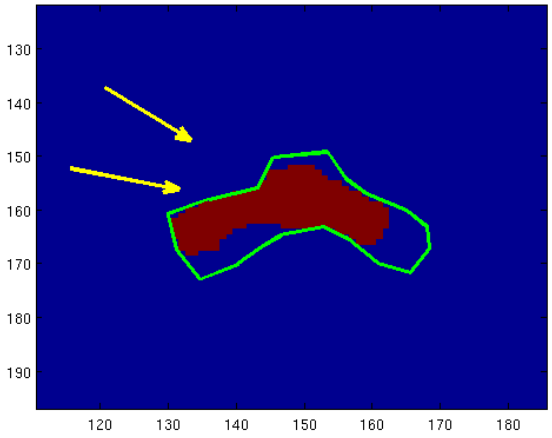

Figure 3.6: Robustness analysis for Solution 2 - The beam angles used were 286 degrees and 304 degrees. Red voxels define the tCTV.

Angles	Average min. dose CTV	Average max. dose CTV
74-88	93% (88,96)	106% (102,118)
286-304	92% (76,95)	108% (104,118)
75-285	**93% (68,96)**	**107% (104,112)**

Table 3.1: The results reflect the CTV coverage. Number in parenthesis are minimal and maximal values obtained form the histograms.

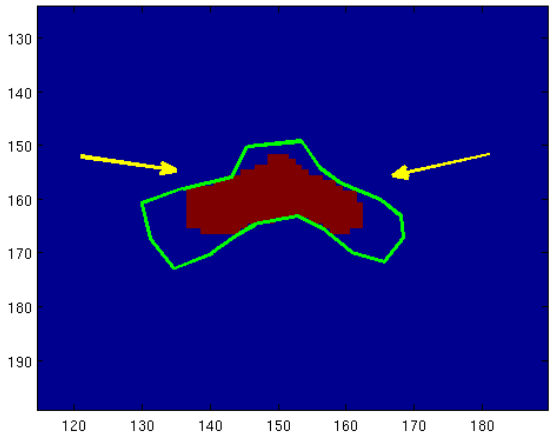

Figure 3.7: Robustness analysis for Solution 3 - The beam angles used were 75 degrees and 285 degrees. Red voxels define the tCTV.

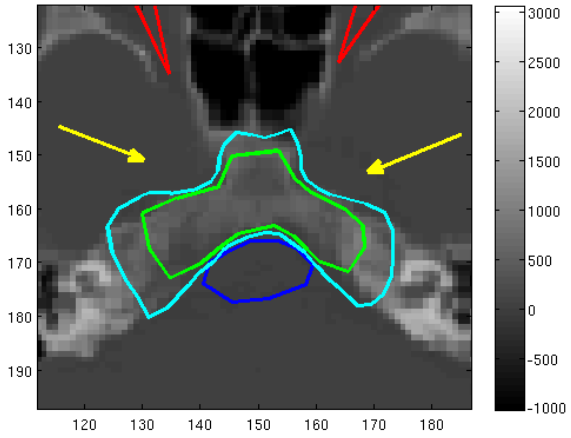

Figure 3.8: PTV expansion for the optimal case - The PTV structure for the optimal case using DTD is shown in cyan.

Angles	Average max. dose OAR	50% isodose volume OAR
74-88	104% (99,108)	96% (93,100)
286-304	106% (101,112)	78% (60,100)
75-285	**98% (96,103)**	**80% (76,88)**

Table 3.2: Results reflect OAR dose impact. Number in parenthesis are minimal and maximal values obtained form the histograms.

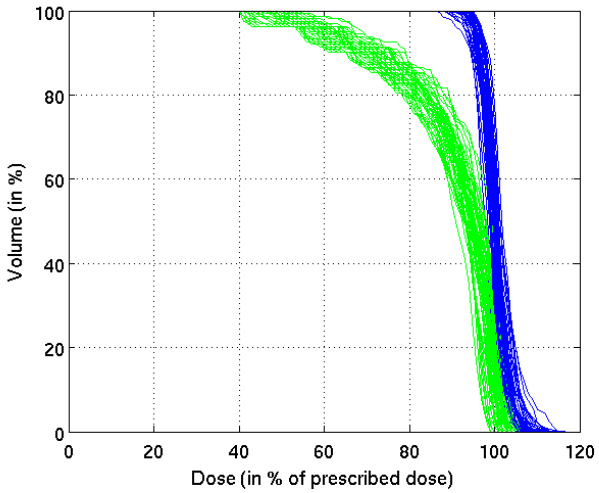

Figure 3.9: Dose Volume Histogram for solution 1 - Only robustness was taken into account. Angles obtained were 88 degrees and 74 degrees. Green lines are the DVHs of OAR, blue lines the DVH of the CTV.

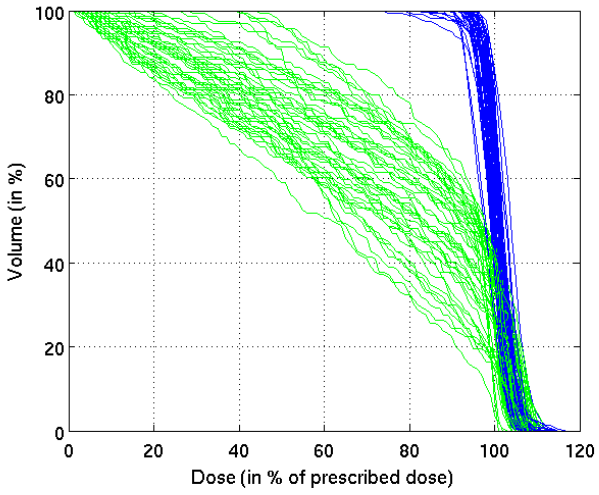

Figure 3.10: Dose Volume Histogram for solution 2 - Directions going through and OAR were avoided. Angles obtained were 286 degrees and 304 degrees. Green lines are the DVHs of OAR, blue lines the DVH of the CTV.

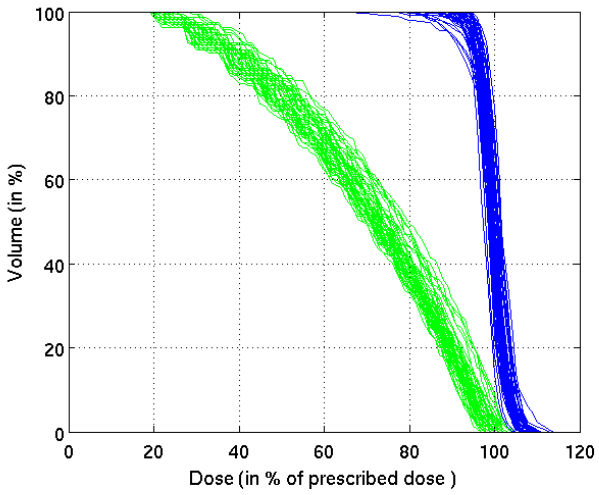

Figure 3.11: Dose Volume Histogram for solution 3 - Directions going through and OAR were avoided and shifts of beam spots near the OAR highly penalized. Angles obtained were 285 degrees and 75 degrees. Green lines are the DVHs of OAR, blue lines the DVH of the CTV.

3.4 Discussion

The motivation for the use of the function R_s as a surrogate of the function R_{tCTV} is based on the fact the it is faster to compute. In fact, while R_{tCTV} requires a histogram of dose calculations the function R_s requires a ray tracing operation for the location of each beam spot. In computing R_s no assumptions whatsoever about Bragg peak degradation or lateral scattering of the particles is made in order to keep the calculation as efficient as possible. One could go one step further and apply the R_s function only to those beam spots that are located in the distal end of the target. This approach was not tried in this work but it is expected to reduced the calculation times since the amount of ray tracing operations would reduce from being proportional to the target volume to being proportional to the projection of the target onto the plane perpendicular to the beam direction.

Obviously the function R_{tCTV} also depends on the values m and v for defining if a voxel is safely treated. We however noticed that for values below 15% the shape of the R_{tCTV} function was nearly the same. We chose values of $m = v = 7\%$ for beam arrangement selection and $m = 5\%, v = 3\%$ for target expansion.

In the platform used for this work (PartPlan) there is a significant difference in time between a dose calculation and a beam spot shift operation. While the dose calculation for protons takes about 3 minutes (for the case shown in this chapter), a beam spot shift is computed within few seconds. For a given direction, a full histogram of beam spot shifts using $N_{max} = 50$ realizations took between one and two minutes.

Although the problem was addressed here using local optimization, it is expected that having a global solver or addressing the issue of the combinatorial character of the problem might improve the results. Having said so the most valuable part of this work is not how the minimization is done from a mathematical point of view but how we have managed to define the problem in harmony with the concept of PTV presented in Chapter 2. Further work aiming to look for global solutions is necessary.

As the reader might have noticed, the number of fields used was predefined by the user. Since their number is usually low (rarely larger than four or five) one could run the algorithm individually for each predefined number of beams.

Another important question is how to expand the method to IMPT plans. It is worth noticing that the functions R_s and R_s^{Max} penalize only beam spot shifts and are not dependent on their intensity. In this sense it is reasonable to think that they will work well for any type of beam spot modulation and preliminary results support this belief, however more work is needed to understand in which scenarios the strategy is adequate and how to merge it with DTD.

4

Conclusions

4.1 Summary

Some of the fundamental ideas of Ion Beam Therapy were introduced in Chapter 1. This introduction was not meant to be a detailed reference of the state-of-art of the field but instead a compact overview of the concepts that were relevant for the following chapters. The technicalities were, for most of the topics, intentionally avoided.

In Chapter 2 the problem of PTV definition in Ion Beam Therapy was addressed. Section 2.1 introduced some of the most relevant concepts used for treatment planning as they are discussed in the ICRU reports 50, 62 and 78(57, 58, 59). In Section 2.2 the convenience of the use of PTV concept as presented in the ICRU 50 was questioned. With counter-examples it was shown that some of the basic requirements for the use of these concepts are not met in Ion Beam Therapy. Section 2.3 proposed new concepts for robust treatment planning in Ion Beam Therapy. These are:

tCTV(m,v): The subvolume of CTV voxels that were not affected by errors and uncertainties.

PTV(m,v): The volume expansion that assures that $tCTV(m, v) = PTV$

Robust Conformity: The concept of conformity in the presence of uncertainties. The indexes R and C, referred to as, *Robust Conformity Indexes* were proposed as quantifiers of robust conformity.

Building on these concepts a novel method for PTV definition was proposed: Dynamic Target Definition (DTD). These ideas were applied and exemplified with a two dimensional Head and Neck case and a two dimensional Prostate case.

Section 2.3.4 discussed the applicability of the PTV concept for IMPT. It was shown that for IMPT the PTV concept by itself does not assure robust CTV dose coverage and a combination of the DTD approach with additional techniques, some of which have been published (69, 70, 71, 72) might help to tackle the problem of robustness for this technique.

Section 2.3.5 presented a framework for treatment planning in Ion Beam Therapy that is developed around the methods and concepts proposed in the previous sections and gives special emphasis on the robustness of the treatment plan.

Chapter 3 focuses on the problem of beam angle selection for Ion Beam Therapy. Section 3.1 discusses the complexity of the problem and explains the strategies commonly found in published algorithms. In Section 3.2 we make a contribution to the problem of beam angle selection in Ion Beam Therapy. Building on the same line of thought we placed *robustness* as the main priority when choosing a beam arrangement. The proposed method builds on the concept of tCTV presented in Chapter 2. We argued that tCTV is a dynamic measure or robustness for a given plan. Based on that we proposed the function

$$R_{tCTV}(\vec{\phi}) = \mu(CTV) - \mu(tCTV) \tag{4.1}$$

as a measure of the merit of a one-beam arrangement. Because this function requires significant computation times we define a secondary function that R_s that behaves in a similar fashion while being much faster to compute. A generalization to a multiple beam arrangement was made through the introduction of the function R_s^{Max}. Finally an strategy to take into account OAR sparing is proposed. It consists of two aspects: avoiding going through OAR and avoiding having high uncertainty regions near the OAR. The first aspect prevents the OAR from receiving low-to-medium doses while the second aspect prevents that uncertainties would have a negative impact on the healthy structure.

These ideas are exemplified in Section 3.3 with a two dimensional Head and Neck case.

4.2 Novelty

The main contribution of this work is to define a conceptual layout to deal with uncertainties in treatment planning with Ion Beams. From this conceptual layout two problems were then addressed: The problem of PTV definition in particle therapy and the problem of beam angle selection. Both questions are considered to be open problems by the international community of particle therapy practitioners and researchers. The methods developed here give at least partial solutions to these problems and allow us to have a better understanding of them.

4.3 Outlook

The work carried out through this thesis has led to a better understanding of some of the challenges of robust treatment planning with Ion Beams. The following aspects remain as problems to be addressed and studied in the future:

4.3.1 IMPT

A combination of the presented methods with robust inverse planning for IMPT is desirable. This will allow us to fully understand the magnitude of the challenges and exploit the benefits of this technique, safely. Some authors have suggested (68) that the traditional PTV concept fails in IMPT. While it is true that conventional methods might not always work in Ion Beam Therapy (as was shown here), the issue with IMPT is robustness. Certain tools might be useful in some situations but generally speaking, if a given plan is highly sensible to errors probably the only countermeasure reasonable is to design a different plan. Having said so we believe that the DTD together with the proposed beam angle selection algorithm and the robust inverse planning work published in the literature (69, 70, 71, 72) will provide a powerful set of tools to navigate through the possibilities of robust inverse planning for IMPT.

4.3.2 Target definition on High LET modalities

The methods developed in this work focused on proton beams delivered with an active system. It was assumed that the RBE was constant along the Bragg Peak. A generalization of the concepts to a non-constant RBE scenario and specially to Carbon Ion

beams is interesting. Although in principle the same methods can be used just by evaluating the RBE-weighted-dose instead of the absorbed dose a more elegant alternative would be to use the concept of *radiobiological effect* instead of the dose. Under this scenario instead of having a histogram of dose distributions one would have a histogram of *effect distributions*[1]. The tCTV would be evaluated by analyzing the fluctuations of the effect in each voxel, just like explained in Chapter 2. This way would also allow to take into consideration the uncertainties of the radiobiological modeling, namely the uncertainties of α and β, if using the LQ model.

The final question to ask would be: "Should CTV-to-PTV expansions be the same for proton and carbon ion plans?"

In addition, it has been shown and discussed in the literature (76, 77, 78) that for protons, the use of a constant RBE might lead to an important underestimation of the effect in the distal part of the beam. Applying the DTD framework with an effect-based-approach would allow us to understand better how distal margins should be defined.

4.3.3 Robust comparison between particle and photon treatments

As medical physicist very often we find ourselves in front of comparisons between photon and ion beam plans which make an effort to show the obvious dosimetric advantage of ion beams as compared to photons. Two or three decades ago, when all proton treatments were done with passive delivery systems and most of the photon treatments were done with old-fashion conventional equipment, there was no discussion that proton therapy had a clear advantage in terms of conformity and integral doses.

However, in the last twenty years photon therapy has had an tremendous revolution in equipment and software. The ability to tailor steep dose gradients near the target has evolved to a point that today it is not a unique feature, anymore, of Ion Beam therapy.

We can go one step further and ask: "How does the *robust conformity* of both modalities compare?". It is clear that in order to make a fair dosimetric comparison between both modalities is not enough to compare nominal plans. For the comparison to be fair one would have to take into account the *degree of belief* attached to a given dose distribution.

[1] In the absence of a better term.

Conducting a study in which the DTD approach is applied to photon and ion beam plans would certainly give us a profound insight on this question.

4.3.4 Clinical implementation

Finally, a clinical implementation of the methods developed in this work is perhaps the most important step to consider. This implementation should probably be carried out in three stages: First it needs to be implemented in the TPS of a facility offering ion beam therapy. After doing so, a study have to be conducted on phantoms to validate the methods and understand their application in a clinical scenario. Finally and assuming the first two stages were successful, the methodology should be deployed into daily clinical practice. This is an ambitious task that would require the commitment and engagement of a large team of people who see the benefits on doing so. The work presented here suggest that by doing so we could provide ion beam treatments that are more robust towards CTV coverage while irradiating "just the right" amount of healthy tissue. This could potentially translate into an enhanced tumor control probability and a reduction of some of the side effects that this kind of therapy usually brings along.

References

[1] R. Bendl, J. Pross, A. Hoess, M. Keller, K. Preiser, and W. Schlegel. **VIRTUOS–A program for VIRTUal radiOtherapy Simulation and verification**. In *Proc 11th Int Conf on the Use of Computers in Radiation Therapy*, 1994. x

[2] G. Cabal and O. Jäkel. **Towards a Probabilistic Approach for PTV Definition in Hadron Therapy**. In *In Proceedings of the XVIth International Conference on the Use of Computers in Radiation Therapy (ICCR)*, 2010. xi

[3] G. Cabal and O. Jäkel. **Towards a novel approach for PTV definition in particle therapy**. *Annual Particle Therapy Cooperative Group Meeting, 2010*, 2010. Gunma, Japan. xi

[4] G. Cabal and O. Jäkel. **Dynamic Target Definition for Ion Beam Therapy**. *Annual Particle Therapy Cooperative Group Meeting, 2011*, 2011. Philadelphia, PE, USA. xi

[5] G. Cabal and O. Jäkel. **Dynamic Target Definition: A novel approach for PTV definition in Ion Beam Therapy**. *Radiother Oncol*, 2011. (conditionally accepted). xi

[6] G. Cabal, S. Luan, and O. Jäkel. **Impact of the beam angle configuration on the quality and the robustness of a particle therapy plan**. *Annual Particle Therapy Cooperative Group Meeting, 2009*, 2009. Heidelberg, Germany, Poster Presentation. xi

[7] G. Cabal, S. Luan, and O. Jäkel. **An algorithm for optimizing beam angle configuration in particle therapy**. *Annual Particle Therapy Cooperative Group Meeting, 2009*, 2009. Heidelberg, Germany, Poster Presentation. xi, 66

[8] RR. Wilson. **Radiological use of fast protons.** *Radiology*, **47**:487–491, 1946. 1, 2, 3, 4

[9] W. Schlegel, T. Bortfeld, and A-L. Grosu, editors. *New technologies in radiation oncology*, page 366. Medical Radiology/Radiation Oncology. Springer, 2006. 2

[10] C. Tobias. **Heavy charged particles in cancer therapy, radiobiology and radiotherapy**, 1967. National Cancer Institute Monograph No. 24. 2

[11] FM. Khan. *The physics of radiation therapy.* Lippincott Williams & Wilkins, third edition edition, 2003. 2

[12] B. Gottschalk. **Passive beam spreading in proton radiation therapy**. http://huhepl.harvard.edu/ gottschalk/. 4, 6

[13] E. Pedroni, R. Bacher, H. Blattmann, T. Bohringer, A. Coray, A. Lomax, G. Lin, G. Munkel, S. Scheib, and U. Schneider. **Proton therapy status reports, PSI Life Sciences Newsletter 1989/1990**, 1989. 4, 5

[14] T. Haberer, W. Becher, D. Schardt, and G. Kraft. **Magnetic scanning system for heavy ion therapy**. *Nucl. Instrum. Methods Phys. Res. A 330*, pages 296–305, 1993. 4, 5

[15] M. Krämer, O. Jäkel, T. Haberer, G. Kraft, D. Schardt, and U. Weber. **Treatment planning for heavy ion radiotherapy: physical beam model and dose optimization.** *Phys Med Biol*, (45):3299–3317, 2000. 6

[16] O. Jäkel, C. Jacob, D. Schardt, CP. Karger, and GH. Hartmann. **Relation between carbon ions ranges and X-ray CT numbers**. *Med Phys*, (28):71–73, 2001. 7, 8, 40, 56

[17] M. Soukup, M. Fippel, and M. Alber. **A pencil beam algorithm for intensity modulated proton therapy derived from Monte Carlo simulations**. *Phys Med Biol*, **50**(21):5089–5104, 2005. 7

[18] H. Szymanowski and U. Oelfke. **Two-dimensional pencil beam scaling: an improved proton dose algorithm for heterogeneous media**. *Phys Med Biol*, **47**(18):3313–3330, 2002. 7, 19

[19] H. Szymanowski and U. Oelfke. **CT calibration for two-dimensional scaling of proton pencil beams**. *Phys Med Biol*, **48**(7):861–874, 2003. 7, 19

[20] H. Paganetti, H. Jiang, SY. Lee, and H. Kooy. **Accurate Monte Carlo for nozzle design, commissioning, and quality assur- ance in proton therapy**. *Med Phys*, **31**:2107–2118, 2004. 7

[21] T. Pawlicki and C. Ma. **Monte Carlo simulation for MLC-based intensity-modulated radiotherapy**. *Med Dosim*, **26**:157–168, 2001. 7

[22] H. Paganetti, H. Jiang, K. Parodi, R. Slopsema, and M. Engelsman. **Clinical implementation of full Monte Carlo dose calculation in proton beam therapy**. *Phys Med Biol*, **53**(17):4825–4853, September 2008. 8

[23] A. Mairani et al. **The FLUKA Monte Carlo code coupled with the local effect model for biological calculations in carbon ion therapy**. *Phys Med Biol*, **55**(15):4273, 2012. 8

[24] A. Lomax. **Intensity modulation methods for proton radiotherapy**. *Phys Med Biol*, **44**:185–205, 1999. 8, 9, 10, 56

[25] JO. Deasy, DM. Shephard, and TR. Mackie. **Distal edge tracking: a proposed delivery method for conformal proton therapy using intensity modulation**. In DD. Leavitt and GS. Starkschall, editors, *Proc. 12th ICCR (Salt Lake City)*. Madison, WI: Medical Physics Publishing, 1997. 9

REFERENCES

[26] H. Paganetti, A. Niemierko, M. Ancukiewicz, LE. Gerweck, M. Goitein, JS. Loeffler, and H. Suit. **Relative biological effectiveness (RBE) values for proton beam therapy**. *Int J Radiat Oncol Biol Phys*, **53**(2):407–421, 2002. 11

[27] T. Kanai et al. **Biophysical characteristics of HIMAC clinical irradiation system for heavy ion radiation therapy**. *Int J Radiat Oncol Biol Phys*, **44**(1):201–210, 1999. 11, 12

[28] CP. Karger, O. Jäkel, M. Scholz, P. Peschke, and J. Debus. **In regard to Dasu and Toma-Dasu, Int J Radiat Oncol Biol Phys 2008;70:867–874**. *Int J Radiat Oncol Biol Phys*, **40**(5):1614–1616, 2008. 13

[29] RB. Hawkins. **A statistical theory of cell killing by radiation of varying linear energy transfer**. *Radiat Res*, **140**(3):366–374, December 1994. 12

[30] RB. Hawkins. **A microdosimetric-kinetic model for the effect of non-Poisson distribution of lethal lesions on the variation of RBE with LET**. *Radiat Res*, **160**(1):61–69, July 2003. 12

[31] JJ. Wilkens and U. Oelfke. **A phenomenological model for the relative biological effectiveness in therapeutic proton beams**. *Phys Med Biol*, **49**(13):2811–2825, July 2004. 12

[32] M. Scholz, AM. Kellerer, W. Kraft-Weyrather, and G. Kraft. **Computation of cell survival in heavy ion beams for therapy. The model and its approximation**. *Radiat Environ Biophys*, **36**:59–66, 1997. 12

[33] T. Elsässer et al. **Quantification of the relative biological effectiveness for ion beam radiotherapy: direct experimental comparison of proton and carbon ion beams and a novel approach for treatment planning**. *Int J Radiat Oncol Biol Phys*, **78**:1177–1183, 2010. 12

[34] CP. Karger et al. **Radiation tolerance of the rat spinal cord after 6 and 18 fractions of photons and carbon ions: experimental results and clinical implications**. *Int J Radiat Oncol Biol Phys*, **66**(5):1488–1497, 2006. 13

[35] U. Oelfke and T. Bortfeld. **Inverse planning for photon and proton beams**. *Med Dosim*, **26**(2):113–124, 2001. 14

[36] S. Nill, T. Bortfeld, and U. Oelfke. **Inverse planning of intensity modulated proton therapy**. *Z Med Phys*, **14**(1):35–40, 2004. 14

[37] J. Llacer, TD. Solberg, and Claus. Promberger. **Comparative behaviour of the Dynamically Penalized Likelihood algorithm in inverse radiation therapy planning**. *Phys Med Biol*, **46**:2637–2663, 2001. 14

[38] LA. Shepp and Y. Vardi. **Maximum likelihood reconstruction for emission tomography**. *IEEE Transactions on Medical Imaging*, **1**(2):113–122, October 1982. 14

[39] JJ. Wilkens and U. Oelfke. **Fast multifield optimization of the biological effect in ion therapy**. *Phys Med Biol*, **51**(12):3127–3140, 2006. 16, 17

[40] M. Zeider and HH. Rossi. **The synergistic effects of different radiations**. *Radiat Res*, **83**:723–739, 1980. 16

[41] AM. Kellerer and HH. Rossi. **A generalized formulation of dual radiation action**. *Radiat Res*, **75**:471–488, 1978. 16

[42] T. Kanai et al. **Irradiation of Mixed Beam and Design of Spread-Out Bragg Peak for Heavy-Ion Radiotherapy**. *Radiat Res*, **147**:78–85, 1997. 16

[43] W. Schneider, T. Bortfeld, and W. Schlegel. **Correlation between CT numbers and tissue parameters needed for Monte Carlo simulations of clinical dose distributions**. *Phys Med Biol*, **45**(2):459–478, 2000. 19

[44] M. Urie, M. Goitein, WR. Holley, and GTY Chen. **Degradation of the Bragg peak due to inhomogeneities**. *Phys Med Biol*, **31**:1–15, 1986. 19, 62

[45] A. Lomax. **Intensity modulated proton therapy and its sensitivity to treatment uncertainties 1: the potential effects of calculational uncertainties**. *Phys Med Biol*, **53**:1027–1043, 2008. 20, 21, 56, 61, 62

[46] M. Bazalova, JF. Carrier, L. Beaulieu, and F. Verhaegen. **Dual-energy CT-based material extraction for tissue segmentation in Monte Carlo dose calculations**. *Phys Med Biol*, **53**(9):2439–2456, 2008. 20

[47] M. Bazalova, JF. Carrier, L. Beaulieu, and F. Verhaegen. **Tissue segmentation in Monte Carlo treatment planning: a simulation study using dual-energy CT images**. *Radiother Oncol*, **86**(1):93–98, 2008. 20

[48] N. Hünemohr et al. **Ion range estimation by using dual energy computed tomography**. (submitted). 20

[49] N. Hünemohr. *Improvement of ion therapy planning by the use of dual energy computed tomography*. Master's thesis, Faculty of Physics and Astronomy, University of Heidelberg, 2011. 20

[50] A. Lomax. **Intensity modulated proton therapy and its sensitivity to treatment uncertainties 2: the potential effects of inter-fraction and inter-field motions**. *Phys Med Biol*, **53**:1043–1056, 2008. 21, 23, 55, 61, 62

[51] CP. Karger et al. **Influence of setup errors on spinal cord dose and treatment plan quality for cervical spine tumours: a phantom study for photon IMRT and heavy charged particle radiotherapy**. *Phys Med Biol*, **48**(19):3171–3189, 2003. 21

[52] C. Bert and E. Rietzel. **4D treatment planning for scanned ion beams**. *Radiat Oncol*, **2**(24), July 2007. 22

[53] C. Bert, SO. Groezinger, and E. Rietzel. **Quantication of interplay effects of scanned particle beams and moving targets**. *Phys Med Biol*, **53**:2253–2265, 2008. 22

[54] C. Bert, A. Gemmel, N. Saito, and E. Rietzel. **Gated irradiation with scanned particle beams**. *Int J Radiat Oncol Biol Phys*, **73**:1270–1275, 2009. 22

[55] T. Furukawa et al. **Moving target irradiation with fast rescanning and gating in particle therapy**. *Med Phys*, **37**:4874–4879, 2010. 22

[56] K. Kraus, E. Heath, and U. Oelfke. **Dosimetric consequences of tumour motion due to respiration for a scanned proton beam**. *Phys Med Biol*, **56**:6563–6581, 2011. 22

[57] **International Commission on Radiation Units and Measurements Report 50: Prescribing, Recording, and Reporting Photon Beam Therapy**, 1993. 24, 26, 28, 46, 55, 56, 77

[58] **International Commission on Radiation Units and Measurements Report 62: Prescribing, Recording and Reporting Proton-beam Therapy (Supplement to ICRU Report 50)**, 1999. 24, 25, 26, 28, 46, 55, 77

[59] **International Commission on Radiation Units and Measurements Report 78: Prescribing, Recording and Reporting Proton-beam Therapy**, 2007. 24, 36, 77

[60] M. van Herk, P. Remeijer, C. Rasch, and JV. Lebesque. **The probability of correct dose coverage: Dose-population histograms for deriving treatment margins in radiotherapy**. *Int J Radiat Oncol Biol Phys*, **47**(4):11121–1135, 2000. 25, 55

[61] M. Van Herk. **Errors and margins in radiotherapy**. *Sem Rad Onc*, **14**(1):52–64, January 2004. 25, 27, 55

[62] J. Purdy. **Current ICRU definitions of volumes: limitations and future directions**. *Sem Rad Onc*, **14**(1):27–40, January 2004. 25, 26, 55

[63] T. Bortfeld, SB. Jiang, and E. Reitzel. **Effects of Motion on the Total Dose Distribution**. *Sem Rad Onc*, **14**(1):41–51, January 2004. 28

[64] WA. Beckham, PJ. Keall, and JV. Siebers. **A fluence-convolution method to calculate radiation therapy dose distributions that incorporate random set-up error**. *Phys Med Biol*, **47**:3465–3473, 2002. 28

[65] M. Engelsman et al. **The effect of breathing and set-up errors on the cumulative dose to a lung tumor**. *Radiother Oncol*, **60**:95–105, 2001. 28

[66] M. Goitein. **Magical protons?** *Int J Radiat Oncol Biol Phys*, **70**(3):654–656, 2008. 35

[67] A. Lomax. **Intensity modulated proton therapy: The potential and the challenge**, 2004. Habilitation thesis. 41, 56

[68] F. Albertini, EB. Hug, and A. Lomax. **Is it necesary to plan with safety margins for actively scanned proton beams?** *Phys Med Biol*, **56**:4399–4413, 2011. 50, 56, 79

[69] J. Unkelbach, TC. Chan, and T. Bortfeld. **Accounting for range uncertainties in the optimization of intensity modulated proton therapy**. *Phys Med Biol*, **52**(10):2755–2773, 2007. 50, 55, 56, 61, 78, 79

[70] J. Unkelbach, T. Bortfeld, BC. Martin, and M. Soukup. **Reducing the sensitivity of IMPT treatment plans to setup errors and range uncertainties via probabilistic treatment planning**. *Med Phys*, **36**(1):149–163, January 2009. 50, 55, 56, 61, 78, 79

[71] D. Pflugfelder, U. Oelfke, and JJ. Wilkens. **Worst case optimization: a method to account for uncertainties in the optimization of intensity modulated proton therapy**. *Phys Med Biol*, **53**(6):1689–1700, 2008. 50, 55, 56, 61, 78, 79

[72] A. Fredriksson, A. Forsgren, and B. Hardemark. **Minimax optimization for handling range and setup uncertainties in proton therapy**. *Med Phys*, **38**:1672–1684, 2011. 50, 55, 56, 61, 78, 79

[73] W. Chen, J. Unkelbach, A. Trofimov, T. Madden, H. Kooy, T. Bortfeld, and D. Craft. **Including robustness in multi-criteria optimization for intensity-modulated proton therapy**. *Phys Med Biol*, **57**(3):591–608, 2012. 55, 61

[74] J. Unkelbach and U. Oelfke. **Incorporating organ movements in inverse planning: Assessing dose uncertainties by Bayesian Inference**. *Phys Med Biol*, **50**(1):121–139, 2005. 55, 58

[75] D. Maleike, J. Unkelbach, and U. Oelfke. **Simulation and visualization of dose uncertainties due to interfractional organ motion**. *Phys Med Biol*, **51**(9):2237–2252, 2006. 55, 58

[76] JB. Robertson et al. **Radiobiological studies of high-energy modulated proton beam utilizing cultured mammalian cells**. *Cancer*, **35**:1664–1677, 1975. 57, 80

[77] H. Paganetti, LE. Gerweck, and M. Goitein. **The general relation between tissue response to x-radiation (values) and relative biological effectiveness (RBE) of protons: prediction by the Katz track-structure**. *Int J Radiat Biol*, **76**:985–998, 2000. 57, 80

[78] A. Carabe et al. **Range uncertainty in proton therapy due to variable biological effectiveness**. *Phys Med Biol*, **57**:1159–1172, 2012. 57, 80

[79] J. Stein et al. **Number and orientations of beams in intensity-modulated radiation treatments**. *Med Phys*, **24**(2):149–160, 1997. 60

[80] T. Bortfeld and W. Schlegel. **Optimization of beam orientations in radiation therapy - some theoretical considerations**. *Phys Med Biol*, **38**:291–304, 1993. 60

[81] A. Pugachev, JG. Li, AL. Boyer, CL. Hancock, QL. Le, SS. Donaldson, and L. Xing. **Role of beam orientation optimization in intensity-modulated radiation therapy**. *Int J Radiat Oncol Biol Phys*, **50**:551–560, 2001. 60

[82] DM. Aleman, A. Kumar, RK. Ahuja, HE. Romeijn, and JF. Dempsey. **Neighborhood search approaches to beam orientation optimization in intensity modulated radiation therapy treatment planning**. *J Glob Optimiz*, **42**:587–607, 2008. 60

REFERENCES

[83] D. Djajaputra, Q. Wu, Y. Wu, and R. Mohan. **Algorithm and performance of a clinical IMRT beam angle optimization system**. *Phys Med Biol*, **48**:3191–3212, 2003. 60

[84] Y. Li, J. Yao, and D. Yao. **Automatic beam angle selection in IMRT planning using genetic algorithm**. *Phys Med Biol*, **49**:1915–1932, 2004. 60

[85] Q. Hou, J. Wang, Y. Chen, and JM. Galvin. **Beam orientation optimization for IMRT by a hybrid method of the genetic algorithm and the simulated dynamics**. *Med Phys*, **30**:2360–2367, 2003. 60

[86] DP. Nazareth, S. Brunner, MD. Jones, HK. Malhotra, and M. Bakhtiari. **Optimization of beam angles for intensity modulated radiation therapy treatment planning using genetic algorithm on a distributed computing platform**. *J Med Phys*, **34**:129–132, 2009. 60

[87] CG. Rowbottom, S. Webb, and S. Oldham. **Beam-orientation customization using an artificial neural network**. *Phys Med Biol*, (44):2251–2262, 1999. 60

[88] X. Wang, X. Zhang, L. Dong, H. Liu, M. Gillin, A. Ahamad, K. Ang, and R. Mohan. **Effectiveness of noncoplanar IMRT planning using a parallelized multiresolution beam angle optimization method for paranasal sinus carcinoma**. *Int J Radiat Oncol Biol Phys*, **63**:594–601, 2005. 60

[89] X. Wang, X. Zhang, L. Dong, H. Liu, Q. Wu, and R. Mohan. **Development of methods for beam angle optimization for IMRT using an accelerated exhaustive search strategy**. *Int J Radiat Oncol Biol Phys*, **60**:1325–1337, 2004. 60

[90] Y. Li, J. Yao, D. Yao, and W. Chen. **A particle swarm optimization algorithm for beam angle selection in intensity-modulated radiotherapy planning**. *Phys Med Biol*, **50**:3491–3514, 2005. 60

[91] WD. D'Souza, HH. Zhang, DP. Nazareth, L. Shi, and RR. Meyer. **A nested partitions framework for beam angle optimization in intensity-modulated radiation therapy**. *Phys Med Biol*, **53**:3293–3307, 2008. 60

[92] M. Bangert and U. Oelfke. **Spherical cluster analysis for beam angle optimization in intensity-modulated radiation therapy treatment planning**. *Phys Med Biol*, **55**(19):6023–6037, 2010. 61

[93] O. Jäkel and J. Debus. **Selection of beam angles for radiotherapy of skull base tumours using charged particles**. *Phys Med Biol*, **45**(5):1229–1242, 2000. 66